G3, 2021, 11(7), jkab134
DOI: 10.1093/g3journal/jkab134
Advance Access Publication Date: 26 April 2021
Investigation

Identification and characterization of rapidly accumulating *sch9*Δ suppressor mutations in *Saccharomyces cerevisiae*

Patricia P. Peterson and Zhengchang Liu *

Department of Biological Sciences, University of New Orleans, New Orleans, LA 70148, USA

*Corresponding author: Department of Biological Sciences, University of New Orleans, 2000 Lakeshore Drive, New Orleans, LA 70148, USA. Email: zliu5@uno.edu

Abstract

Nutrient sensing is important for cell growth, aging, and longevity. In *Saccharomyces cerevisiae*, Sch9, an AGC-family protein kinase, is a major nutrient sensing kinase homologous to mammalian Akt and S6 kinase. Sch9 integrates environmental cues with cell growth by functioning downstream of TORC1 and in parallel with the Ras/PKA pathway. Mutations in *SCH9* lead to reduced cell growth in dextrose medium; however, reports on the ability of *sch9*Δ mutants to utilize non-fermentable carbon sources are inconsistent. Here, we show that *sch9*Δ mutant strains cannot grow on non-fermentable carbon sources and rapidly accumulate suppressor mutations, which reverse growth defects of *sch9*Δ mutants. *sch9*Δ induces gene expression of three transcription factors required for utilization of non-fermentable carbon sources, Cat8, Adr1, and Hap4, while *sch9*Δ suppressor mutations, termed *sns1* and *sns2*, strongly decrease the gene expression of those transcription factors. Despite the genetic suppression interactions, both *sch9*Δ and *sns1* (or *sns2*) homozygous mutants have severe defects in meiosis. By screening mutants defective in sporulation, we identified additional *sch9*Δ suppressor mutants with mutations in *GPB1*, *GPB2*, and *MCK1*. Using library complementation and genetic analysis, we identified *SNS1* and *SNS2* to be *IRA2* and *IRA1*, respectively. Furthermore, we discovered that lifespan extension in *sch9*Δ mutants is dependent on *IRA2* and that PKA inactivation greatly increases basal expression of *CAT8*, *ADR1*, and *HAP4*. Our results demonstrate that *sch9*Δ leads to complete loss of growth on non-fermentable carbon sources and mutations in *MCK1* or genes encoding negative regulators of the Ras/PKA pathway reverse *sch9*Δ mutant phenotypes.

Keywords: Sch9; Ira1/2; Mck1; Gpb1/2; respiratory metabolism

Introduction

In eukaryotic cells, physiological adaptations to changes in the internal and external environments are regulated by dynamic signal transduction networks that are generally conserved throughout evolution. For *Saccharomyces cerevisiae*, nutrient availability is the major environmental factor driving cell growth and survival (reviewed in Schuller 2003; Zaman *et al.* 2008; Turcotte *et al.* 2010; Loewith and Hall 2011; Broach 2012). Yeast cells utilize interconnected signaling pathways and transcriptional regulatory networks to respond to the external supply of nutrients and adjust their growth and metabolism. Carbon and nitrogen nutrients in particular serve as both substrates to support cell growth and as signaling molecules to guide cellular processes necessary for survival. An important mediator of this coordinated response is the protein kinase Sch9, which functions in both glucose and nitrogen sensing pathways.

Sch9 is a member of the AGC family of serine/threonine protein kinases and is a homolog of mammalian Akt/Protein Kinase B and ribosomal protein (RP) S6 kinase (S6K). Several AGC-family protein kinases are phosphorylated and activated by the evolutionarily conserved Target of Rapamycin (TOR) kinase, a major regulator of cell growth and metabolism in response to environmental signals (Wullschleger *et al.* 2006). Akt is directly phosphorylated in its hydrophobic motifs by mammalian TOR complex 2 (mTORC2) in response to hormones and other growth factors. Another well-characterized AGC-family kinase is S6K, which is phosphorylated in its hydrophobic motifs and activated by mTORC1 (Burnett *et al.* 1998) to stimulate ribosomal biogenesis (Ribi) and protein synthesis. In yeast, Sch9 was identified as a major downstream effector of TORC1 signaling and functional ortholog of S6K or PKB/Akt1 (Geyskens *et al.* 2001; Sobko 2006; Urban *et al.* 2007). Sch9 is directly phosphorylated in its C-terminal hydrophobic motifs and an adjacent site by TORC1 and in its activation loop by the yeast PDK1 orthologs Pkh1 and Pkh2. When nitrogen is abundant or preferred nitrogen sources are not limiting, TORC1 is activated and promotes mass accumulation and cell growth by inducing ribosome biosynthesis, which is achieved partly through the activation of Sch9 (reviewed in Loewith and Hall 2011). Sch9 positively regulates the expression of genes in Ribi and RP regulons by phosphorylating repressors Dot6, Tod6, and Stb3 and thereby inhibiting the recruitment of the RPD3L histone deacetylase complex to target gene promoters (Urban *et al.* 2007; Huber *et al.* 2009; Lee *et al.* 2009; Lippman and Broach 2009; Huber *et al.* 2011). Sch9 also positively regulates RNA polymerase III-dependent transcription of 5S ribosomal RNA and tRNA genes by directly phosphorylating and inhibiting Maf1, as well as RNA polymerase I-dependent expression of 35S pre-ribosomal RNA (Huber *et al.* 2009; Lee *et al.* 2009; Wei and Zheng 2009).

Received: January 14, 2021. **Accepted:** April 14, 2021
Published by Oxford University Press on behalf of Genetics Society of America 2021. This work is written by US Government employees and is in the public domain in the US.

In addition to its functions in the TORC1-mediated nitrogen sensing branch of nutrient signaling, Sch9 may also play a role in the regulation of cell growth in response to the quality of carbon sources. Glucose-grown cells exhibit an increase in both protein level and phosphorylation of Sch9 (Jorgensen *et al.* 2004; Urban *et al.* 2007). There has been much evidence to suggest that Sch9 functions in a pathway parallel to cAMP-dependent protein kinase PKA and that the two kinases exhibit some functional redundancy (reviewed in Loewith and Hall 2011; Broach 2012). *SCH9* was originally identified as a multicopy suppressor of growth defects associated with loss of Ras or PKA activity and, conversely, hyperactivation of PKA due to *TPK1* overexpression, *bcy1*Δ, or expression of a constitutive activating mutant of *RAS2*, $RAS2^{Val19}$, suppresses the slow growth defects of *sch9*Δ strain (Toda *et al.* 1988; Prusty and Keil 2004). The activity of PKA is regulated by cAMP, whose synthesis depends on the activity of adenylate cyclase (reviewed in Thevelein and de Winde 1999; Broach 2012). PKA is a tetramer of two identical regulatory subunits encoded by *BCY1* and two catalytic subunits encoded by the three functionally redundant genes, *TPK1*, *TPK2*, and *TPK3*. cAMP activates PKA by binding to Bcy1, relieving its inhibition of the catalytic subunits. Activation of PKA is positively regulated by the G protein-coupled receptor Gpr1 and its associated Gα protein, Gpa2 (Kraakman *et al.* 1999; Lorenz *et al.* 2000). Adenylate cyclase activity is also mediated by Ras proteins Ras1 and Ras2, which are regulated positively by Cdc25, the guanine nucleotide exchange factor of Ras, and negatively by Ira1 and Ira2, the GTPase-activating proteins of Ras. Two other related proteins, Gpb1 and Gpb2, also negatively regulate the activity of the Ras/PKA signaling pathway (Harashima and Heitman 2002; Harashima *et al.* 2006; Budhwar *et al.* 2011). Gpb1 promotes ubiquitin-dependent proteolysis of Ira2 and Gpb2 inhibits Ras activity through direct interactions with Ira1 and Ira2 (Harashima *et al.* 2006; Phan *et al.* 2010). PKA stimulates cell growth in part by inhibiting transcription factors Msn2/4 and Gis1, which regulate the expression of stress-responsive element- and post-diauxic shift-driven genes, respectively, and Rim15, a protein kinase that induces progression into stationary phase and meiosis (reviewed in Roosen *et al.* 2005; Broach 2012). Despite the suggested functional redundancy with PKA, the role of Sch9 in glucose sensing is still unclear. On one hand, 90% of the glucose-induced changes in gene expression can be recapitulated by PKA activation or Sch9 overexpression in glycerol-grown cells. On the other hand, Sch9 inactivation does not interfere with the glucose response, while PKA inactivation does (Zaman *et al.* 2009). The common substrates of Sch9 and PKA include Dot6, Tod6, and Maf1, which are important factors for the regulation of ribosome synthesis and the expression of tRNA genes (Huber *et al.* 2009; Lee *et al.* 2009; Lippman and Broach 2009; Soulard *et al.* 2010; Huber *et al.* 2011). Sch9 and PKA have similar phosphorylation site motifs and share overlapping target substrates (Plank *et al.* 2020), which helps to explain their close relationship in mediating cell growth and survival in response to nutrient signals.

Consistent with its role as an important kinase sensing nutrient and stress conditions, Sch9 has been implicated in many cellular processes. Sch9 is involved in the regulation of stress-responsive genes (Pedruzzi *et al.* 2003; Roosen *et al.* 2005; Lavoie and Whiteway 2008). Inhibition of both Sch9 and PKA is known to induce autophagy (Yorimitsu *et al.* 2007). Sch9 negatively regulates the expression of genes in the nitrogen discrimination pathway (Smets *et al.* 2008), which are controlled by several GATA transcription factors including Gln3 and Gat1 (Cooper 2002; Smets *et al.* 2008). Interestingly, a *gln3 gat1* double mutation confers resistance to rapamycin treatment and partially suppresses the growth defects of *sch9*Δ mutant cells (Schmelzle *et al.* 2004; Urban *et al.* 2007). Sch9 and PKA converge on Rim15 to regulate transcription of genes involved in the stress response and during the post diauxic shift (Pedruzzi *et al.* 2003; Roosen *et al.* 2005). Sch9 regulates both chronological and replicative life span (Morano and Thiele 1999; Fabrizio *et al.* 2001, 2003; Kaeberlein *et al.* 2005), which is partly mediated by Rim15 (Fabrizio *et al.* 2001; Wei *et al.* 2008; Burtner *et al.* 2009). Sch9 has also been shown to regulate cell size, osmotic stress response, sphingolipid metabolism, ceramide biosynthesis, V-ATPase assembly, and pH homeostasis (Jorgensen *et al.* 2002; Pascual-Ahuir and Proft 2007; Swinnen *et al.* 2014; Wilms *et al.* 2017). Together, the evidence suggests that Sch9 participates in a dynamic signaling network to regulate cell growth and survival in response to nutrient and stress conditions.

Sch9 and its eukaryotic homologs are broadly implicated in integrating extracellular and intracellular signals to promote cell growth and survival. It is compelling to understand the functions and regulatory mechanisms of Sch9. There are currently discrepancies in the literature with regards to how *sch9* mutations impact cells' ability to utilize non-fermentable carbon sources. Sch9 mutations have been reported to cause a range of severe to no growth defects on non-fermentable carbon sources (Crauwels *et al.* 1997; Jorgensen *et al.* 2004; Roosen *et al.* 2005; Lavoie and Whiteway 2008; Zhang *et al.* 2011; Teixeira *et al.* 2014). There are also conflicting reports about the effects that *sch9* mutations have on the expression of genes encoding mitochondrial proteins, the *HAP4* gene, which encodes the regulatory subunit of the Hap2/3/4/5 transcription factor complex, and stress-responsive genes such as *HSP12* and *HSP26* (Fabrizio *et al.* 2003; Roosen *et al.* 2005; Lavoie and Whiteway 2008; Smets *et al.* 2008; Pan and Shadel 2009; Pan *et al.* 2011; Teixeira *et al.* 2014). These discrepancies could be due to fast accumulation of *sch9*Δ suppressor mutations, originally reported by Huber et al. (2009) who used analog-sensitive *sch9* alleles instead of *sch9*Δ to minimize complications that may be caused by *sch9*Δ suppressor mutations. Nevertheless, many published results were generated using *sch9*Δ mutant strains.

Here, we report the isolation and characterization of spontaneous and rapidly accumulating suppressor mutations that occur in slow-growing *sch9*Δ mutant cells. We found that *sch9*Δ cells are unable to grow on non-fermentable carbon sources in two commonly used strain backgrounds, W303-1A and W303-1B as well as BY4741 and BY4742. The suppressor mutations rescue the growth defects of *sch9*Δ mutants on both dextrose medium and non-fermentable carbon sources. We found that mutations in *IRA1* and *IRA2* account for all of the spontaneous, recessive *sch9*Δ suppressor mutations that were isolated. We further found that mutations in *GPB1*, *GPB2*, and *MCK1* can suppress the growth defects of *sch9*Δ mutant cells. We also show that PKA negatively regulates the expression of *CAT8*, *ADR1*, and *HAP4*. Altogether, we have identified genes responsible for spontaneous *sch9*Δ suppressor mutations that may complicate the analysis of the cellular functions of Sch9.

Materials and methods

Strains, plasmids, growth media, growth conditions, and yeast transformation

Yeast strains and plasmids used in this study are listed in Tables 1 and 2, respectively. Yeast strains were grown at 30° in YPD (1% Bacto-yeast extract, 2% Bacto-peptone; and 2% glucose),

Table 1 Yeast strains used in this study

Strain	Genotype	Source	Application
BY4741	*MATa his3Δ1 leu2Δ0 met17Δ0 ura3Δ0*	Lab. stock	Figures 2B, 3, 4, 5, 6C, and 7
BY4742	*MATα his3Δ1 leu2Δ0 lys2Δ0 ura3Δ0*	Lab. stock	Figure 2A
W303-1A	*MATa ura3-1 ade2-1 leu2-3,112 trp1-1 his3-11,15*	Lab. stock	Figures 1 and 3D
W303-1B	*MATα ade2-1, his3-11, 15, ura3-1, leu2-3, 112, trp1-1, can1-100*	Lab. stock	Figure 3D
PPY566	BY4741 *sch9Δ::kanMX4 sns1*	This study	Figures 2A and 3B
ZLY6649	BY4741 *sch9Δ::kanMX4*	This study	Figures 2B, 4D, 5B, and 5C
ZLY6650	BY4741 *sch9Δ::kanMX4*	This study	Figures 4C, 4E, 5C, and 8
PPY730	BY4741 *sns1*	This study	Figures 2B and 3B
PPY733	BY4741 *sch9Δ::kanMX4 sns1*	This study	Figures 2B and 5D
PPY632	BY4741 *sch9Δ::kanMX4*	This study	Figures 3B, 4F, and 5E
PPY633	BY4742 *sch9Δ::kanMX4*	This study	For constructing PPY745
PPY731	BY4742 *sns1*	This study	For constructing PPY737
PPY734	BY4742 *sch9Δ::kanMX4 sns1*	This study	For constructing PPY741
BY4743	BY4741 × BY4742	This study	Figures 2C, 3, 4A, 5, and 8
PPY745	PPY632 × PPY633	This study	Figures 2C, 3, 4A, 5A, 5D, and 8
PPY737	PPY730 × PPY731	This study	Figures 2C, 3, 4A, and 8
PPY741	PPY733 × PPY734	This study	Figures 2C, 3, 4A, 5A, and 8
PPY624	W303-1B *MATα sch9Δ::kanMX4*	This study	Figures 1 and 3D
PPY673	W303-1A *MATa sch9Δ::kanMX4 sns1*	This study	Figure 1
PPY622	W303-1A *MATa sch9Δ::kanMX4*	This study	Figure 3D
ZLY6614	BY4741 *sns2*	This study	Figures 2B, 3C, and 4A
ZLY6619	BY4741 *sch9Δ::kanMX4 sns2*	This study	Figures 2, A, B, 3C, 4A, and 5D
ZLY6626	BY4742 *sch9Δ::kanMX4 sns2*	This study	Figures 4A and 5D
ZLY6581	BY4742 *sns2*	This study	Figure 4A
ZLY6519	BY4741 *isc1Δ::kanMX4*	This study	Figure 4B
ZLY6606	BY4741 *mck1Δ::kanMX4*	This study	Figure 4, B–F
ZLY6609	BY4741 *ira2Δ::kanMX4*	This study	Figure 5, B and E
ZLY6629	BY4741 *get2Δ::kanMX4*	This study	Figure 4B
ZLY6634	BY4742 *vma6Δ::kanMX4*	This study	Figure 4B
ZLY6633	BY4742 *paf1Δ::kanMX4*	This study	Figure 4B
ZLY6637	BY4741 *atg15Δ::kanMX4*	This study	Figure 4B
ZLY6640	*MATα his3Δ1 leu2Δ0 ura3Δ0 met17Δ0 def1Δ::kanMX4*	This study	Figure 4B
ZLY6642	BY4742 *tps2Δ::kanMX4*	This study	Figure 4B
ZLY6644	BY4741 *dep1Δ::kanMX4*	This study	Figure 4B
ZLY6645	BY4742 *sem1Δ::kanMX4*	This study	Figure 4B
ZLY6647	BY4741 *ira1Δ::kanMX4*	This study	Figure 5E
ZLY6662	BY4741 *vac8Δ::kanMX4*	This study	Figure 4B
ZLY6665	BY4742 *erv14Δ::kanMX4*	This study	Figure 4B
ZLY6669	BY4741 *vma2Δ::kanMX4*	This study	Figure 4B
ZLY6604	BY4741 *gpb2Δ::kanMX4*	This study	Figures 4, B, C, E, and F
ZLY6660	*MATa his3Δ1 leu2Δ0 lys2Δ0 ura3Δ0 met17Δ0 sch9Δ::kanMX4 ira2Δ::kanMX4*	This study	Figure 5E
ZLY6661	BY4741 *sch9Δ::kanMX4 ira2Δ::kanMX4*	This study	Figure 5, B and D
ZLY6601	BY4742 *ira2Δ::kanMX4*	This study	Figure 5B
ZLY6648	BY4742 *ira1Δ::kanMX4*	This study	Figure 5C
ZLY6651	BY4742 *sch9Δ::kanMX4*	This study	Figure 4C
ZLY6602	BY4742 *gpb2::kanMX4*	This study	Figure 4C
ZLY6652	BY4741 *sch9Δ::kanMX4 mck1Δ::kanMX4*	This study	Figure 4, D and F
PPY754	*MATa his3Δ1 leu2Δ0 lys2Δ0 ura3Δ0 met17Δ0 sch9Δ::kanMX4 ira1Δ::kanMX4*	This study	Figure 5C
PPY755	BY4742 *sch9Δ::kanMX4 ira1Δ::kanMX4*	This study	Figure 5, D and E
PPY734	BY4742 *sch9Δ::kanMX4 sns1*	This study	Figure 5D
PPY777	*MATα his3Δ1 leu2Δ0 lys2Δ0 ura3Δ0 met17Δ0 sch9Δ::kanMX4 gpb1Δ::kanMX4*	This study	Figure 4F
PPY757	BY4741 *gpb1Δ::kanMX4*	This study	Figure 4, C, E, and F
ZLY6677	BY4742 *sch9Δ::kanMX4 gpb2Δ::kanMX4*	This study	Figure 4, C, E, and F
PPY763	*MATa his3Δ1 leu2Δ0 lys2Δ0 ura3Δ0 gpb1Δ::kanMX4 gpb2Δ::kanMX4*	This study	Figure 4, E and F
PPY767	BY4741 *sch9Δ::kanMX4 gpb1Δ::kanMX4 gpb2Δ::kanMX4*	This study	Figure 4, E and F
ZLY4313	BY4741 *yak1Δ::kanMX4*	This study	Figures 6 A, B, and 7A
ZLY5023	BY4741 *yak1Δ::HIS3 tpk1Δ::kanMX4 tpk2Δ::kanMX4 tpk3Δ::kanMX4*		Figure 6, A and B
ZLY6715	BY4741 *bcy1Δ::kanMX4*	This study	Figure 6C
PPY776	*MATa his3Δ1 leu2Δ0 lys2Δ0 ura3Δ0 pde1Δ::kanMX4 pde2Δ::kanMX4*	This study	Figures 6C and 7B
ZLY6578	BY4743 *ira2Δ/IRA2*	Yeast genome	Figure 5B
ZLY6656	BY4743 *ira1Δ/IRA1*	deletion project	Figure 5C
ZLY6707	BY4741 *sch9Δ::kanMX4 yak1Δ::kanMX4*	This study	Figure 7A
ZLY4368	BY4741 *pde2Δ::kanMX4*	This study	Figure 7B
PPY758	BY4741 *sch9Δ::kanMX4 pde2Δ::kanMX4*	This study	Figure 7B

YPL [1% Bacto-yeast extract, 2% Bacto-peptone and 3.7% DL-lactic acid (w/w, 85%), adjusted to pH 5.3 using NaOH], YPEG (1% Bacto-yeast extract, 2% Bacto-peptone, 2% ethanol, and 3% glycerol), minimal dextrose medium (SD) (0.67% yeast nitrogen base and 2% glucose), YPR (1% Bacto-yeast extract, 2% Bacto-peptone, and 2% raffinose), sporulation media (0.1% Bacto-yeast extract, 1% potassium acetate, and 0.02% raffinose), YNBcasD or YNBcas5D (0.67% yeast nitrogen base, 0.25% casamino acids, 2% or 5% dextrose), YNBcasR (0.67% yeast nitrogen base, 0.25% casamino acids, and 2% raffinose), or YNBcasL [0.67% yeast nitrogen

TABLE 2 Plasmids used in this study

Plasmid	Description	Reference	Application
pDC115	pHAP4-lacZ, expressing *lacZ* under the control of a 1.8kbp *HAP4* promoter.	This study	Figures 3, A–D, 4, B, F, 5E, and 6
pZL2140	pCAT8-lacZ, expressing *lacZ* under the control of an 866 bp *CAT8* promoter.	This study	Figures 3, A–D, and 6
pZL2108	pADR1-lacZ, expressing *lacZ* under the control of a 1249 bp *ADR1* promoter.	This study	Figures 3, A–D, and 6
pZL3929	pRS416-CAT8-HA, encoding Cat8 with a C-terminal 3xHA tag under the control of the endogenous promoter.	This study	Figure 3, E and G
pZL1324	pRS416-HAP4-HA, encoding Hap4 with a C-terminal 3xHA tag under the control of the endogenous promoter.	This study	Figure 3, F and H
pZL2416	YCp50	Lab. stock	Figure 5A
pPP322	YCp50-lib., a *sns1*-complementing library plasmid encoding *IRA2* and *REX4*.	This study	Figure 5A

base, 1% casamino acids, and 3.7% DL-lactic acid, adjusted to pH 5.3] as indicated. Amino acids, adenine, and uracil were added to the growth medium at standard concentrations to cover auxotrophic requirements if needed (Amberg *et al.* 2005). Agar was added to a final concentration of 2% to solidify growth medium. For transformation, yeast cells were freshly grown in YPD media and transformed with plasmids using the high-efficiency method (Gietz *et al.* 1992).

Yeast cell extract preparation, Ponceau S staining, and Western blotting

Total cellular proteins were prepared by treating yeast cells with a freshly made solution of 7.5% β-mercaptoethanol and 1.85 N NaOH and precipitated with trichloroacetic acid as described previously (Yaffe and Schatz 1984). Protein samples were resuspended in SDS-PAGE sample buffer with 100 mM dithiothreitol and boiled for three minutes before being separated by SDS-PAGE. Pre-stained protein ladder (broad range, 10–230 kDa, P7710S, New England Biolabs) was used in protein gels. Proteins were transferred to a nitrocellulose membrane for immunoblotting with monoclonal anti-HA antibody, clone 3F10. HRP-conjugated secondary antibody from Jackson ImmunoResearch Laboratories (West Grove, PA) was used to probe the primary antibody. Membranes were stained in 0.1% Ponceau S in 0.1% acetic acid for 10 minutes and images of Ponceau-stained membranes were taken before immunoblotting. Chemiluminescence images of Western blots were captured using the Bio-Rad ChemiDoc MP imaging system and processed using Bio-Rad Image Lab software. Protein bands on Western blots were quantified using the same software.

β-Galactosidase assays

Yeast strains were grown at 30° to mid-log phase for at least six generations to reach an optical density at 600 nm (OD_{600}) of 0.6–0.8. Cells were collected by centrifugation and β-galactosidase activity assays were conducted as described previously (Amberg *et al.* 2005). Assays were carried out in duplicate for each sample from three independent cultures. β-galactosidase activities were given as the mean ± SD, $n = 3$.

Chronological lifespan assay

Yeast cultures (two replicates per sample) were grown in YPR media with a starting OD_{600} of 0.01 and allowed to grow until cells reached stationary phase (two days for wild type, *sns1*, and *sch9Δ sns1* strains; four days for *sch9Δ* mutant strain), which was set to be day 0 for the lifespan assay. Cultures were removed from the flask every five days starting from day 0 and live cells were quantified by colony forming assay. For colony forming assay, 500 cells from each culture were plated on YPD plates and colony forming units (CFUs) were counted and averaged after 3 days' growth at 30°. The percentage of viable cells relative to day 0 (100% survival) was calculated and plotted. The values are the mean ± SD of two independent experiments.

Sporulation efficiency assay

Diploid strains were grown on SD plate for 2 days and then transferred into 1 ml sporulation media with starting OD_{600} of 0.3. After eight days of incubation with shaking at 220 rpm at 30°, 400 total cells were counted for each independent strain and the percentage of cells that had formed dyads and tetrads was recorded. The data were generated from the results of three replicate samples per strain.

Data availability

The authors affirm that all data necessary to draw conclusions in this article are present within the texts, figures, and tables. Strains, plasmids, and other noncommercial research reagents are available upon request.

Results

sns1 and *sns2* mutations reverse the growth defects of *sch9Δ* mutants on both dextrose and non-fermentable carbon sources

sch9Δ mutations have been reported to cause a range of severe to no growth defects in cells grown on non-fermentable carbon sources. To understand the discrepancies reported in the literature, we generated a heterozygous *sch9Δ* mutation in the W303 strain background and obtained *sch9Δ* mutants via tetrad analysis. Figure 1A shows that each tetrad yielded two big wild type and two small *sch9Δ* mutant colonies on dextrose medium, consistent with published results (Toda *et al.* 1988; Lorenz *et al.* 2000). W303 background strains have an *ade2* mutation, leading to a red colony phenotype on solid dextrose medium. The smaller *sch9Δ* mutant colonies were white, suggesting *sch9Δ* may lead to defects in respiratory metabolism. When *sch9Δ* mutant cells were streaked onto a dextrose medium plate, fast-growing red colonies appeared among the small white *sch9Δ* mutant colonies (Figure 1B). These large red *sch9Δ* mutant colonies were suspected to contain suppressor mutations. Upon further propagation on plates, the number of fast-growing suppressor mutant colonies quickly surpassed that of slow-growing *sch9Δ* mutant colonies. To quantify the growth phenotypes of *sch9Δ* mutants and the suppressor mutants, we performed a serial dilution growth assay of a wild type strain, an *sch9Δ* single mutant, and an *sch9Δ sns1* (*sch9 suppressor 1*) double mutant on both a fermentable carbon source, dextrose, and non-fermentable carbon sources, lactate, and ethanol/glycerol. Figure 1C shows *sch9Δ* mutants have growth defects on dextrose and show no growth on the lactate and ethanol/glycerol plates except for putative

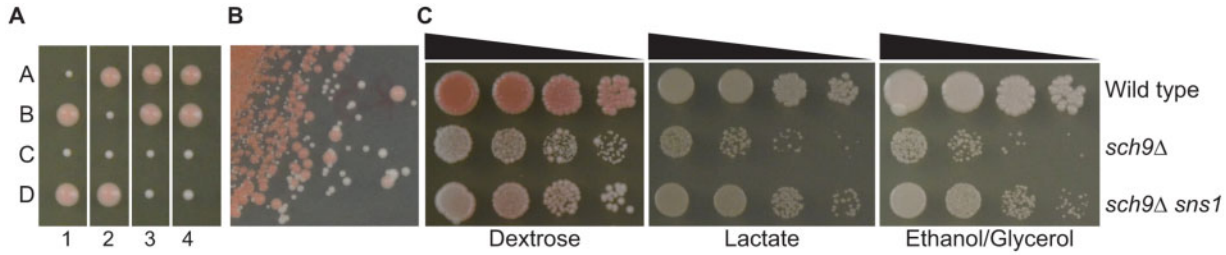

Figure 1 *sch9Δ* mutant cells in the W303 background have growth defects and rapidly accumulate suppressor mutations. (A) Tetrad analysis of wild type (W303-1A) × *sch9Δ* (PPY624) on YPD plate medium. Each tetrad, numbered 1-4, was dissected into four spores labeled A-D. (B) *sch9Δ* mutants quickly accumulate suppressor mutations. An *sch9Δ* mutant strain (PPY624) was streaked on YPD plate. Small white colonies are *sch9Δ* mutants, while large red colonies are *sch9Δ* mutants carrying suppressor mutations. (C) The growth defects of *sch9Δ* mutants are suppressed by a *sns1* mutation. Wild type (W303-1A), *sch9Δ* (PPY624), and *sch9Δ sns1* (PPY673) mutant strains were serially diluted and spotted on YPD (Dextrose), YPL (Lactate), and YPEG (Ethanol/Glycerol) medium.

suppressor mutant colonies. However, the *sns1* mutation partially suppresses the growth defects of *sch9Δ* mutant cells on both dextrose and non-fermentable carbon sources. Our data indicate that the growth defects of *sch9Δ* mutant cells from the W303 background can be reversed by a high frequency of spontaneous suppressor mutations.

BY4741 and closely related strains are derived from the S288c background, which were used in the yeast genome deletion project and are commonly utilized in yeast research labs. We wanted to determine whether *sch9Δ* suppressor mutations would also be easily and spontaneously obtained in this strain background. We generated *sch9Δ* mutants in S288c background strains by both direct transformation with an *sch9Δ::kanMX4* disruption cassette and tetrad analysis. Similar results were obtained: *sch9Δ* results in a slow growth phenotype on dextrose medium and spontaneous suppressor mutations arise at a high frequency. A high frequency of *sch9Δ* suppressor mutations could skew some of the reported phenotypes of *sch9Δ* mutants and mask the cellular functions of Sch9. As such, it was difficult for us to maintain *sch9Δ* mutant cells free of suppressor mutants in both W303 and S288c background strains. Therefore, it is important to know the identity of genes whose spontaneous mutation suppresses *sch9Δ*. To that end, we isolated 21 *sch9Δ* suppressor mutants from both W303 and S288c backgrounds. These *sch9Δ sns* double mutants were crossed to *sch9Δ* mutant cells and the resultant diploid strains were analyzed for growth defects on both dextrose and glycerol medium. Based on their growth phenotypes, three of the 21 mutant strains were found to carry dominant *sch9Δ* suppressor mutations and were not analyzed further. We conducted a complementation group analysis on the remaining 18 mutant strains carrying recessive *sch9Δ* suppressor mutations. Accordingly, *sch9Δ* suppressor mutant strains of opposite mating types were crossed to generate diploids and analyzed for their ability to grow on glycerol plates. All resultant diploid strains were homozygous for *sch9Δ* and would display a *sch9Δ* suppressor mutant phenotype if the two haploid strains carried mutations in the same gene. From our analysis, we placed the 18 recessive *sch9Δ* suppressor mutations into two complementation groups, which were designated *sns1* and *sns2*.

To further characterize the *sch9Δ* suppressor mutations, we performed tetrad analysis on wild type × *sch9Δ sns1* and wild type × *sch9Δ sns2* diploid strains (Figure 2A). As in the W303 background strains, *sch9Δ* mutant colonies from the S288c background were slow-growing on dextrose medium. *sns1* and *sns2* single mutant colonies on the dissection plate exhibited a slight growth defect compared with the wild type and had a rough edge or "papillae" phenotype. In the *sch9Δ sns1* and *sch9Δ sns2* double mutant colonies, *sns1* and *sns2* suppressed the slow growth of *sch9Δ* and yielded colonies of a similar size to wild type. Interestingly, the double mutant colonies appeared to have a relatively smooth edge like wild type, suggesting that *sch9Δ* suppresses the papillae phenotype of *sns1* and *sns2* mutants.

We performed serial dilution growth assays to quantify the suppression of *sch9Δ* by *sns1* and *sns2* (Figure 2B). On both dextrose medium and non-fermentable carbon sources, lactate and ethanol/glycerol, *sns1* and *sns2* single mutants grew like wild type. On dextrose medium, both *sns1* and *sns2* mutations fully suppressed the slow growth phenotype of *sch9Δ* mutant cells. On non-fermentable carbon sources, *sch9Δ* mutant cells did not exhibit any growth, except for a few presumed suppressor mutant colonies, while the *sns1* and *sns2* mutations completely reversed the growth defect of *sch9Δ* mutant cells. It often took several trials to get serial dilution growth assay results from *sch9Δ* mutant strains with no or a small number of suppressor mutants. Since most of the suppressor mutants carried recessive mutations, we decided to test the growth phenotype in diploid strains with the expectation that spontaneous suppressor mutants would be less likely to arise in the diploid setting. To that end, we generated an *sch9Δ* × *sch9Δ* homozygous diploid strain and found they showed a lower frequency of suppressors. *sch9Δ* suppression by *sns1* was also observed in serial dilutions of the diploid strains (Figure 2C). When cells were left on dextrose medium for seven days, wild type colonies developed a tan color while *sch9Δ* mutant cells were white. Yeast cells without mitochondrial DNA, also known as rho0 petites, are unable to grow on non-fermentable carbon sources and form completely white colonies on plate. The white colony phenotype of *sch9Δ* mutant cells is consistent with their inability to grow on non-fermentable carbon sources. DAPI staining of *sch9Δ* cells showed that mitochondrial DNA maintenance did not seem to be affected. Furthermore, diploid cells formed between the crossing of *sch9Δ* mutant cells and a rho0 strain without mitochondrial DNA were able to grow on non-fermentable carbon sources, indicating that *sch9Δ* mutant cells have functional mitochondrial DNA and thus are not mitochondrial petites. Since the identities of *SNS1* and *SNS2* were not known at this stage of our study, we looked for other unique phenotypes of *sns1* and *sns2* mutants. Interestingly, washing of the plate surface with water after seven days of cell growth on dextrose medium showed that the *sns1/sns1* and *sch9Δ/sch9Δ sns1/sns1* diploid strains displayed increased agar adhesion (Figure 2C). The same phenotype was also observed for haploid *sns1*, *sns2*, *sch9Δ sns1*, and *sch9Δ sns2* mutant strains. Together, these results indicate that the growth defects of *sch9Δ* mutants on both dextrose and non-fermentable carbon sources are reversed by spontaneously

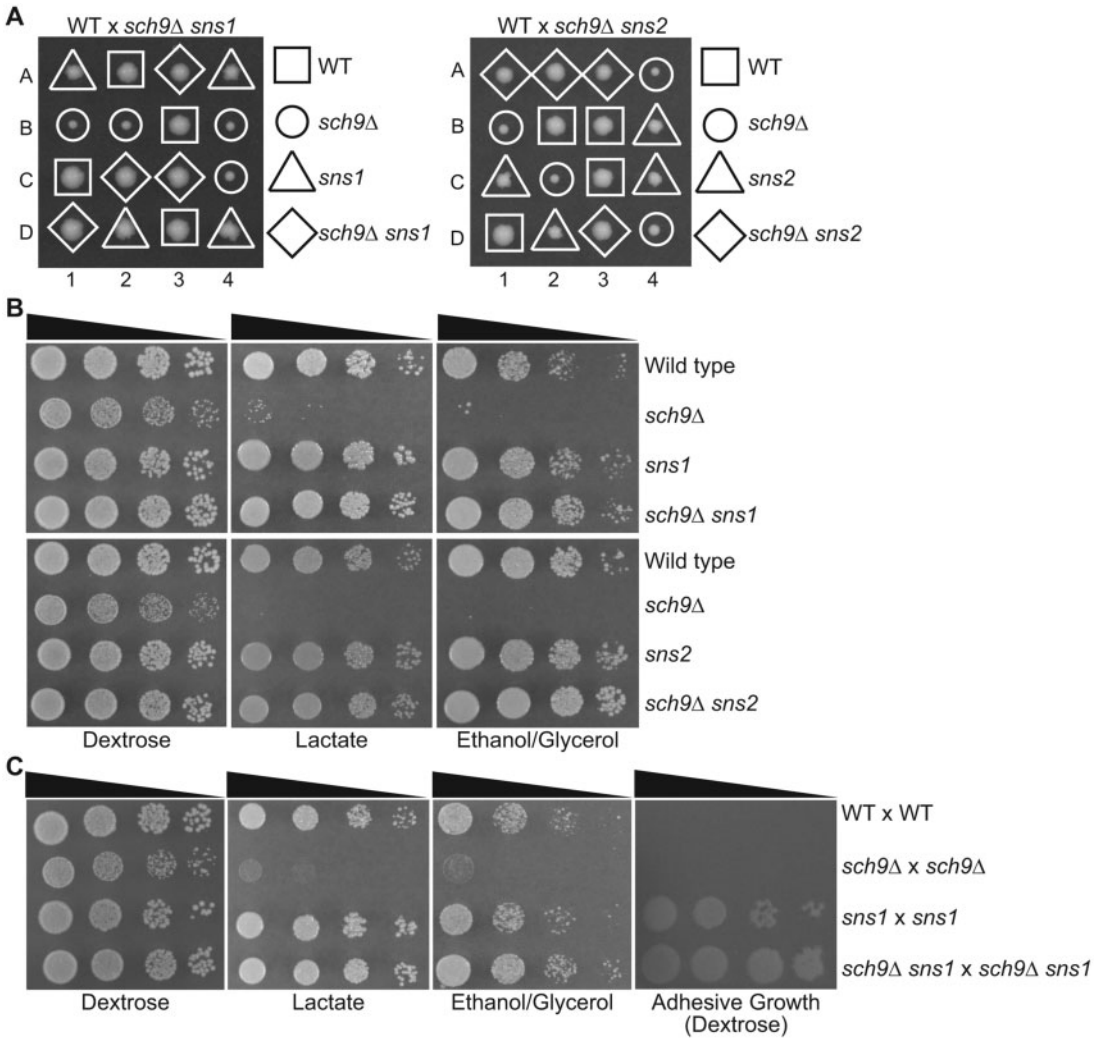

Figure 2 *sns1* and *sns2* mutations reverse growth defects of *sch9***Δ** mutants in the S288c background. (A) Tetrad analysis of wild type (BY4742) × *sch9***Δ** *sns1* (PPY566) and wild type (BY4742) × *sch9***Δ** *sns2* (ZLY6619) on YPD plates. (B) Wild type (BY4741) and isogenic *sch9***Δ** (ZLY6649), *sns1* (PPY730), *sns2* (ZLY6614), *sch9***Δ** *sns1* (PPY733), and *sch9***Δ** *sns2* (ZLY6619) mutant strains were serially diluted and spotted on YPD (Dextrose), YPL (Lactate), and YPEG (Ethanol/Glycerol) medium. (C) Wild type (WT × WT) (BY4741 × BY4742) and isogenic *sch9***Δ** × *sch9***Δ** (PPY745), *sns1* × *sns1* (PPY737), and *sch9***Δ** *sns1* × *sch9***Δ** *sns1* (PPY741) mutant strains were serially diluted and spotted on YPD, YPL, and YPEG plates. Adhesive growth of strains on dextrose medium was examined by washing the agar surface with a stream of water. The plate was photographed shortly after being washed.

arising *sns1* and *sns2* mutations and that *sns1* and *sns2* mutants exhibit similar phenotypes.

*sch9*Δ and *sns1* mutations have opposing effects on the expression of genes encoding transcription factors Cat8, Adr1, and Hap4

Utilization of non-fermentable carbon sources requires transcriptional activators that regulate the expression of genes involved in both respiratory metabolism and gluconeogenesis. Cat8 and Adr1 are involved in the derepression of genes required for growth on non-fermentative carbon sources, while the Hap2/3/4/5 complex is a master regulator of mitochondrial biogenesis and respiratory metabolism (reviewed in Turcotte *et al.* 2010). It has been reported that Sch9 is a positive regulator of *ADH2* expression, which requires Adr1 (Denis and Audino 1991). Reports on the effects of *sch9* mutations on *HAP4* expression were inconsistent (Roosen *et al.* 2005; Lavoie and Whiteway 2008). Discrepancy on the growth phenotype of *sch9***Δ** mutant cells on non-fermentable carbon sources in the published studies and ours prompted us to examine the role of Sch9 in the regulation of Hap4, Cat8, and Adr1. Accordingly, we generated *lacZ* reporter genes under the control of the *CAT8*, *ADR1*, and *HAP4* promoters and examined their expression in wild type and *sch9***Δ** mutant cells grown in dextrose as well as in raffinose medium. Raffinose was chosen because it allows *sch9***Δ** mutant cells to grow and is a glucose-limiting carbon source, which is expected to lead to similar changes in gene expression to those in cells grown in non-fermentable carbon source media. Studies on the regulation of the retrograde signaling pathway in which rho0 cells without mitochondrial DNA were grown in raffinose medium to study gene expression under glucose derepression conditions have been successful (Liu and Butow 1999). The expression of *HAP4*, *ADR1*, and *CAT8* are subject to glucose repression (Forsburg and Guarente 1989; Hedges *et al.* 1995; Dombek and Young 1997; Randez-Gil *et al.* 1997). Consistently, Figure 3A shows that all three reporter genes exhibit higher activity in raffinose-grown wild type cells compared with dextrose. In S288c, background strains grown in dextrose and raffinose media, both the haploid and homozygous diploid *sch9***Δ** mutant strains showed an increase in all three reporter genes compared with the wild type haploid and diploid strains,

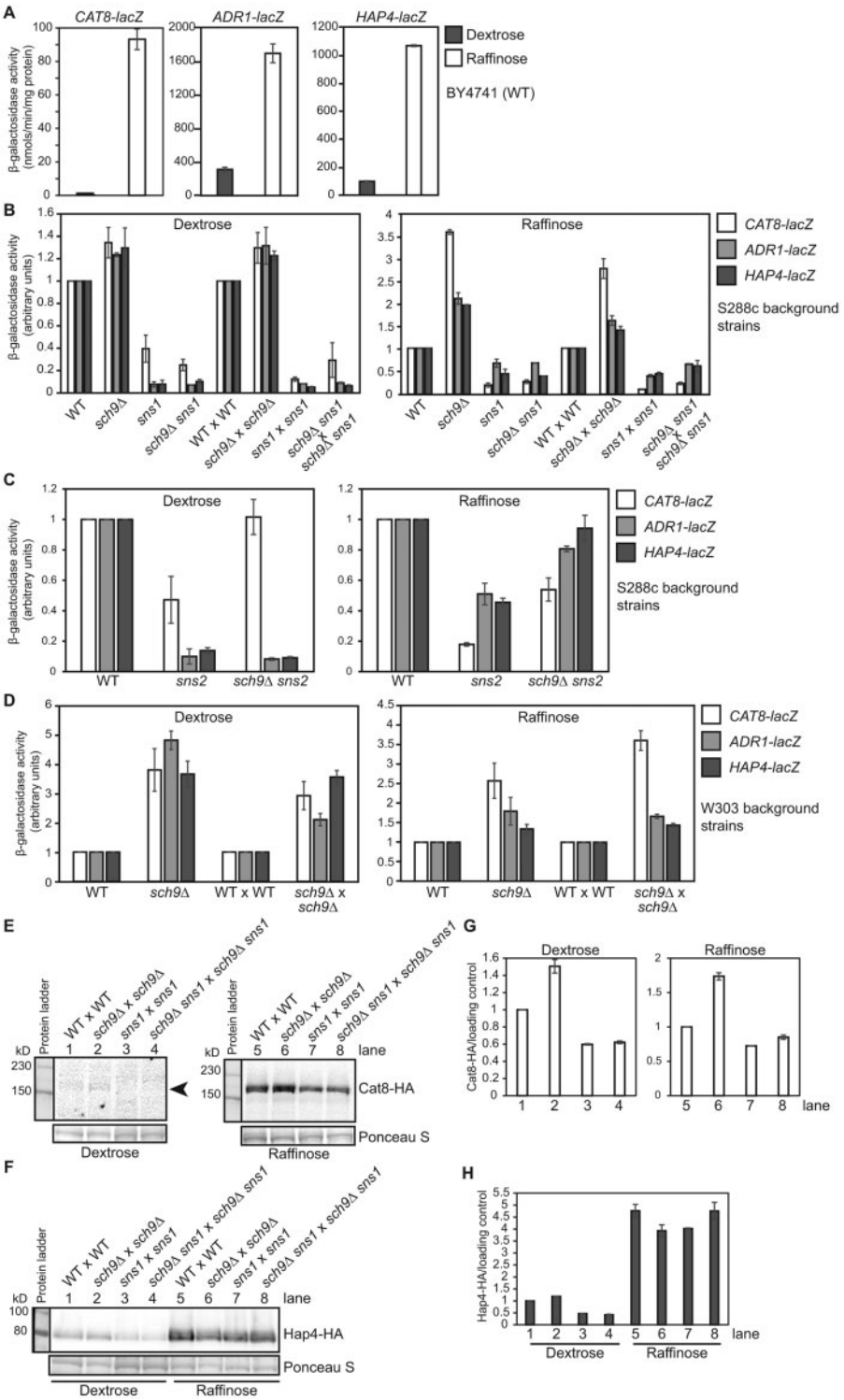

Figure 3 *sch9*Δ and *sns1* mutations have opposing effects on the expression of *CAT8*, *ADR1*, and *HAP4*. (A) β-galactosidase activities of *CAT8-lacZ*, *ADR1-lacZ*, and *HAP4-lacZ* reporter genes in the BY4741 wild type strain grown in YNBcas5D (Dextrose) and YNBcasR (Raffinose) medium. β-galactosidase activity assays were carried out as described in Materials and Methods. (B) β-galactosidase activities of *CAT8-lacZ*, *ADR1-lacZ*, and *HAP4-lacZ* reporter genes in haploid wild type (WT, BY4741), *sch9*Δ (PPY632), *sns1* (PPY730), and *sch9*Δ *sns1* (PPY566) mutant strains and corresponding diploid strains (WT × WT, PPY745, PPY737, PPY741) grown in YNBcas5D and YNBcasR medium. The reporter gene activity in wild type haploid and diploid strains grown in dextrose and raffinose medium was set as 1, respectively. (C) β-galactosidase activities of *CAT8-lacZ*, *ADR1-lacZ*, and *HAP4-lacZ* reporter genes in haploid wild type (WT, BY4741), *sns2* (ZLY6614), and *sch9*Δ *sns2* (ZLY6619) mutant strains grown in YNBcas5D and YNBcasR medium. (D) β-galactosidase activities of *CAT8-lacZ*, *ADR1-lacZ*, and *HAP4-lacZ* in the W303 background strains. Wild type haploid (W303-1B), *sch9*Δ mutant haploid (PPY622), wild type diploid (W303-1A × W303-1B), and *sch9*Δ homozygous mutant diploid cells (PPY622 × PPY624) were grown in YNBcas5D or YNBcasR. (E and F) Western blots of Cat8-HA and Hap4-HA in wild type and mutant diploid strains as indicated. Wild type (BY4741 × BY4742), *sch9*Δ × *sch9*Δ (PPY745), *sns1* × *sns1* (PPY737), and *sch9*Δ *sns1* × *sch9*Δ *sns1* (PPY741) mutant strains carrying a plasmid encoding *CAT8-HA* (pZL3929) (panel E) or *HAP4-HA* (pZL1324) (panel F) were grown in YNBcas5D and YNBcasR medium. The left and right panels of Cat8-HA were from the same membrane, but the Western blot from dextrose-grown cells required a longer exposure time due to weak signals. The arrowhead indicates the position of Cat8-HA bands. Ponceau S staining was used as the loading control. (G and H) Quantification of the ratios of Cat8-HA (panel G) and Hap4-HA (panel H) protein amount to the loading control by Ponceau S staining. The ratio of HA-tagged protein/loading control was set as 1 in wild type cells. The data are presented as the mean ± standard deviation, n = 2.

respectively (Figure 3B). The *sns1* mutation had an opposite effect on the expression of *CAT8, ADR1*, and *HAP4* and exhibited a significant decrease in β-galactosidase activity compared with the wild type. *sch9Δ sns1* double mutant strains, like *sns1* single mutants, also showed reduced expression of these three reporter genes compared with the wild type in both dextrose- and raffinose-grown cells (Figure 3B). The effect of *sns2* on the expression of these three reporter genes was similar to that of *sns1* (Figure 3C). To address whether the difference in reporter gene activity was strain dependent, we also performed β-galactosidase assays on these three reporter genes in wild type and isogenic *sch9Δ* strains in the W303 background and found that *sch9Δ* increased the expression of the three reporter genes in cells grown in both dextrose and raffinose media (Figure 3D). In this strain background in dextrose media, *sch9Δ* leads to an even more significant 3.6 to 4.8-fold increase in *CAT8, ADR1*, and *HAP4* expression in the haploid strains and a 2.1- to 3.6-fold increase in the diploid strains. In raffinose-grown W303 background strains, an increase in reporter gene activity due to *sch9Δ* was comparable with what was observed for the S288c background strains.

To address whether changes in gene expression are reflected in changes in the protein level, plasmids encoding functional C-terminal HA-tagged Hap4 and Cat8 were generated and transformed into wild type, *sch9Δ*, *sns1*, and *sch9Δ sns1* diploid strains of the S288c background and HA-tagged proteins were analyzed by Western blotting. Figure 3, E and G shows that *sch9Δ* increased the expression of Cat8-HA in both dextrose- and raffinose-grown cells and that *sns1* and *sch9Δ sns1* mutants exhibited reduced expression of Cat8-HA compared with wild type. *sch9Δ* and *sns1* increased and decreased the protein level of Hap4-HA in dextrose-grown cells, respectively (Figure 3, F and H). Their effect on Hap4-HA expression is largely absent in raffinose-grown cells, which is somewhat consistent with the smaller effect of *sch9Δ* and *sns1* on *HAP4-lacZ* expression compared with their effect on *CAT8-lacZ* expression in diploid cells (Figure 3B, right panel). It is possible that Hap4-HA protein expression was subject to a saturation effect due to its much higher expression level in raffinose-grown cells than *CAT8* (Figure 3A).

Mutations in *MCK1* and *GPB1/GPB2* partially suppress *sch9Δ*

Since the identities of *SNS1* and *SNS2* were thus far unknown, we looked for *sns1* and *sns2* mutant phenotypes that might be useful in cloning *SNS1* and *SNS2*. *sns1* and *sns2* mutants displayed other phenotypes, including the formation of papillae and tanner-colored colonies, increased adhesive growth, prominent vacuolar structures, and larger cell size (Figure 2, A and C, and data not shown). Phenotypes that are helpful in library complementation such as growth defects at high or low temperatures, or sensitivity to drugs such as caffeine, were not found for *sns1* mutants.

During our genetic analysis of *sch9Δ* mutants, we found that an *sch9Δ* homozygous diploid mutant showed reduced tetrad formation by 7.7-fold compared with wild type (Figure 4A). Since *sns1* and *sns2* mutations reverse the growth defects of *sch9Δ* mutant cells, we asked whether they would also suppress sporulation defects. Instead, however, the introduction of *sns1* and *sns2* mutations further reduced efficiency of tetrad formation, suggesting that mutations in *SNS1* and *SNS2* may have their own sporulation defects. Indeed, both *sns1* and *sns2* homozygous mutant strains showed almost no tetrad formation. Two large-scale studies have been conducted to identify genes required for sporulation (Deutschbauer *et al.* 2002; Enyenihi and Saunders 2003). We decided to use the sporulation phenotype to identify *SNS1* and *SNS2*. Accordingly, we chose 85 genes from the study by Enyenihi and Saunders (2003) and seven genes that showed both a genetic or physical interaction with *SCH9* and sporulation defects when mutated (curated data from the *Saccharomyces* genome database). Since *HAP4-lacZ* expression was greatly reduced in both *sns1* and *sns2* single mutant cells, we hypothesized that *HAP4-lacZ* reporter gene expression could be used to narrow down the list of 92 genes by looking for genes that showed reduced expression of *HAP4-lacZ* when mutated. Accordingly, we transformed a *HAP4-lacZ* reporter gene into these 92 haploid mutant strains obtained from the yeast genome deletion project and the resulting transformants were analyzed for β-galactosidase activity. We found mutations in *ATG15, DEF1, DEP1, ERV14, GPB2, GET2, ISC1, MCK1, PAF1, SEM1, TPS2, VAC8, VMA2*, and *VMA6* reduced *HAP4-lacZ* expression by at least threefold. We then generated these 14 mutant strains via tetrad analysis from respective heterozygous mutant strains obtained from the yeast genome deletion project. Re-examination of *HAP4-lacZ* expression confirmed that *HAP4-lacZ* expression was reduced by at least twofold in 10 of the 14 mutants (Figure 4B). We crossed each of the 14 mutant strains with an *sch9Δ* mutant and obtained respective double mutant strains via tetrad analysis. Analysis of colony size on the dissection plates revealed that mutations in *MCK1* and *GPB2* partially suppressed the growth defects due to *sch9Δ*, which was confirmed by serial dilution growth assays (Figure 4, C, D, and E). Interestingly, mutations in *MCK1* and *GPB2* also caused the largest decreases in *HAP4-lacZ* expression among the 14 mutants (Figure 4B). A large decrease in *HAP4-lacZ* expression was observed in *sns1* and *sns2* mutant cells (Figure 3, B and C). Together, our data suggest that reduced *HAP4* expression correlates with *sch9Δ* suppression.

Mck1 is a protein kinase of the glycogen synthase kinase-3 family, which has three other members in budding yeast, Mds1, Ygk3, and Mrk1 (Bianchi *et al.* 1993; Puziss *et al.* 1994; Hardy *et al.* 1995; Hirata *et al.* 2003). Mck1 and Ygk3 are paralogs, sharing 43% sequence identity and 64% sequence similarity. We generated an *sch9Δ ygk3Δ* double mutant via tetrad analysis and found that *ygk3Δ* did not suppress the growth defects of *sch9Δ*. We then generated *sch9Δ mck1Δ ygk3Δ* triple mutant strains and compared their growth phenotype with *sch9Δ mck1Δ* double mutants. We found their growth was indistinguishable. These results suggest that *sch9Δ* suppression by *mck1Δ* is not shared by *ygk3Δ*.

Gpb2 is a negative regulator of the Ras/PKA signaling pathway and has a paralog Gpb1 (Harashima and Heitman 2002; Broach 2012). We crossed a *gpb1Δ* mutant with an *sch9Δ* mutant and obtained *sch9Δ gpb1Δ* double mutant strains via tetrad analysis. We found *gpb1Δ* marginally suppressed the growth defect of *sch9Δ* mutant cells (Figure 4C, lower left panel). Nevertheless, tetrad analysis revealed the growth defects of *sch9Δ* mutant cells on dextrose medium are almost completely suppressed by a *gpb1/2Δ* double mutation (Figure 4C, lower right panel). We performed a serial dilution growth assay on *sch9Δ gpb1Δ* double mutant strains and found they accumulated suppressor mutations to a greater extent than *sch9Δ* mutant cells. This prevented us from drawing a definitive conclusion on whether there was weak suppression of *sch9Δ* by *gpb1Δ*. However, Figure 4E shows that a *gpb1/2Δ* double mutation suppresses the growth defects of *sch9Δ* mutants better than a *gpb2Δ* single mutation on both dextrose medium and nonfermentable carbon sources. Together, these results indicate that *GPB1* and *GPB2* play a redundant role in inhibiting cell growth in *sch9Δ* mutant cells, with *GPB2* playing a bigger role than *GPB1*.

We examined *HAP4-lacZ* expression in *sch9Δ mck1Δ*, *gpb1Δ*, *sch9Δ gpb1Δ*, *sch9Δ gpb2Δ*, and *sch9Δ gpb1/2Δ* mutant cells grown

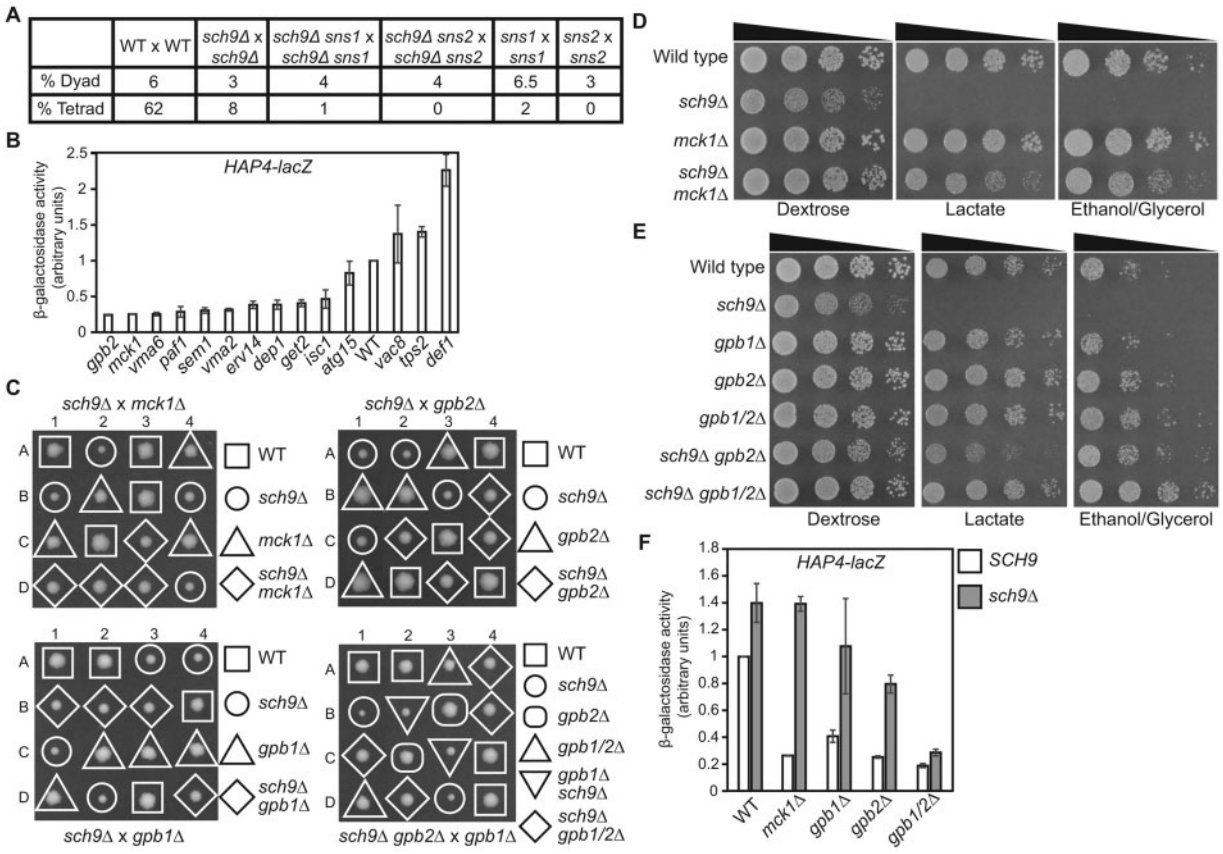

Figure 4 Mutations in *MCK1* and *GPB1/2* suppress the growth defects of *sch9Δ* mutant cells. (A) Mutations in *SCH9*, *SNS1*, and *SNS2* lead to severe sporulation defects. Frequency of dyads and tetrads in the indicated isogenic diploid strains was calculated after eight days of growth in sporulation media. WT × WT, BY4741 × BY4742; *sch9Δ* × *sch9Δ*, PPY745; *sch9Δ sns1* × *sch9Δ sns1*, PPY741; *sch9Δ sns2* × *sch9Δ sns2*, ZLY6619 × ZLY6626; *sns1* × *sns1*, PPY737; *sns2* × *sns2*, ZLY6581 × ZLY6614. (B) β-galactosidase activities of a *HAP4-lacZ* reporter gene in haploid wild type and 14 deletion mutant strains in genes whose mutation leads to sporulation defects in homozygous mutant cells. Cells were grown to mid-log phase in YNBcas5D medium and assayed for β-galactosidase activities. (C) Tetrad analysis of *sch9Δ* (ZLY6651) crossed with *mck1Δ* (ZLY6606), *gpb1Δ* (PPY757), or *gpb2Δ* (ZLY6604), and *sch9Δ gpb2Δ* (ZLY6677) × *gpb1Δ* (PPY757) on YPD plates. Each dissected tetrad, numbered 1-4, yielded four spores, labeled A-D. (D) Wild type (BY4741) and isogenic *sch9Δ* (ZLY6649), *mck1Δ* (ZLY6606), and *sch9Δ mck1Δ* (ZLY6652) mutant strains were serially diluted and spotted on YPD, YPL, and YPEG plates. (E) Wild type (BY4741) and isogenic *sch9Δ* (ZLY6650), *gpb1Δ* (PPY757), *gpb2Δ* (ZLY6604), *gpb1/2Δ* (PPY763), *sch9Δ gpb2Δ* (ZLY6677), and *sch9Δ gpb1/2Δ* (PPY767) mutant strains were serially diluted and spotted on YPD, YPL, and YPEG plates. (F) β-galactosidase activities of *HAP4-lacZ* in wild type (BY4741) and isogenic *mck1Δ* (ZLY6606), *gpb1Δ* (PPY757), *gpb2Δ* (ZLY6604), and *gpb1/2Δ* (PPY763) mutant strains with or without an *sch9Δ* mutation grown in YNBcas5D medium. The *HAP4-lacZ* reporter gene activity in the wild type strain is set as 1.

in dextrose medium. We found that increased expression of *HAP4-lacZ* due to *sch9Δ* is not affected by *mck1Δ*, is partially reduced by *gpb2Δ*, and is almost completely reversed by a *gpb1/2Δ* double mutation (Figure 4F). *gpb1Δ* single and *gpb2Δ* single mutations reduced *HAP4-lacZ* expression by 2.5-fold and fourfold, respectively, while a *gpb1/2Δ* double mutation reduced *HAP4-lacZ* expression by 5.3-fold. The large error bar of *HAP4-lacZ* activity in *sch9Δ gpb1Δ* likely reflects fast accumulation of other suppressor mutations, which could reduce *HAP4-lacZ* expression as observed in *sch9Δ sns1* and *sch9Δ sns2* mutant cells. Taken together, there seems to be a correlation between suppression of *sch9Δ* mutant growth defects and the extent of reduction in *HAP4-lacZ* expression due to *gpb1Δ*, *mck1Δ*, *gpb2Δ*, *gpb1/2Δ*, *sns1*, and *sns2* mutations. *mck1Δ*, *gpb1Δ*, *gpb2Δ*, and *gpb1/2Δ* mutant colonies did not have a clear papillae phenotype like *sns1* and *sns2* mutants. Therefore, *SNS1* and *SNS2* are unlikely to be *MCK1*, *GPB1*, or *GPB2*.

IRA1 and *IRA2* play a largely non-redundant role in *sch9Δ* suppression

Alongside our genetic screening of mutant genes that lead to sporulation defects, we sought to clone the *SNS1* gene by direct complementation using a yeast genomic DNA library. Our first attempt was to use the color phenotype of W303 background strains, as *sch9Δ* cells with an *ade2* mutation leads to small white colonies, while *sch9Δ sns1* double mutant cells form red colonies (Figure 1). We transformed *sch9Δ sns1* double mutant cells with a yeast genomic DNA library and looked for transformants that were white, which would indicate complementation of *sns1*. We conducted several rounds of transformation and recovered many white colonies, none of which contained a *sns1* complementing plasmid. We hypothesized that spontaneous mutations might complicate library plasmid complementation of *sch9Δ* in haploid strains. Accordingly, we used *sch9Δ*/*sch9Δ sns1*/*sns1* diploid mutant cells in the S288c background and transformed them with a yeast genomic DNA library. In this strain background, we expected that *sch9Δ sns1* transformants containing a complementing *SNS1* plasmid would display *sch9Δ* mutant phenotypes of slow growth on dextrose medium and no growth on non-fermentable carbon sources. Of the approximate 12,000 transformants on dextrose medium, dozens of colonies that were slow-growing were chosen for further analysis. Transformant colonies were then examined for severe growth defects on glycerol medium. We found one transformant that showed plasmid-dependent growth defects. We recovered the plasmid from the

transformant, re-transformed it into the *sch9Δ/sch9Δ sns1/sns1* mutant cells, and found that the library plasmid could complement the *sns1* mutation (Figure 5A). Sequencing of the *sns1*-complementing plasmid found that it carried a ~15kb chromosomal DNA fragment, which included complete coding sequences of *IRA2* and *REX4*, and partial coding sequences of *ATG19* and *AVO1*.

ira2 mutant cells have been reported to exhibit increased adhesive growth and sporulation defects (Tanaka *et al.* 1990b; Barrett *et al.* 2012). Our data showed that *sns1* mutants also had sporulation defects and inceased agar adhesion (Figures 2C and 4A), suggesting *IRA2*, not *REX4*, complements the *sns1* mutation. During dissection of tetrads from sporulated *IRA2/ira2Δ* cells, we observed that *ira2Δ* mutant colonies grew slower than wild type and formed papillae, rough-edged colonies (Figure 5B, left panel), similar to *sns1* colonies (Figure 2A, left panel), suggesting *IRA2* is *SNS1*. We then crossed an *ira2Δ* mutant with an *sch9Δ* mutant and obtained *sch9Δ ira2Δ* double mutant strains via tetrad analysis (Figure 5B, middle panel). A serial dilution growth assay showed that *ira2Δ* completely suppressed the growth defects of *sch9Δ* mutant cells on both dextrose and non-fermentable carbon sources (Figure 5B, right panel). *IRA2* has a paralog, *IRA1*. We conducted similar genetic analyses and found that the phenotypes of *ira1Δ* mutants are similar to those of *ira2Δ* mutants and that *ira1Δ* also completely suppressed the growth defects of *sch9Δ* mutant cells (Figure 5C).

We next sought to determine whether *IRA1* is *SNS2*. We crossed mutant strains among *sch9Δ sns1*, *sch9Δ sns2*, *sch9Δ ira1Δ*, and *sch9Δ ira2Δ* mutants and analyzed cell growth of the resultant diploid strains via a serial dilution growth assay. Figure 5D shows that *sch9Δ ira1Δ* × *sch9Δ sns2* and *sch9Δ ira2Δ* × *sch9Δ sns1* diploid strains exhibited similar growth to wild type on both dextrose and lactate medium, suggesting that *IRA1* is *SNS2* and *IRA2* is *SNS1*. *sch9Δ ira1Δ* × *sch9Δ ira2Δ*, *sch9Δ ira1Δ* × *sch9Δ sns1*, and *sch9Δ ira2Δ* × *sch9Δ sns2* diploid strains grew slightly better than *sch9Δ/sch9Δ* homozygous mutant, but still exhibited clear growth defects. This result is somewhat surprising. Ira1 and Ira2 are homologous proteins and play a partially redundant role in inhibiting the activity of Ras1 and Ras2. On the one hand, loss of both copies of *IRA1* or *IRA2* can restore growth of *sch9Δ/sch9Δ* mutant cells to wild type level. On the other hand, loss of one copy each of *IRA1* and *IRA2* only partially suppresses the growth defects of *sch9Δ/sch9Δ* mutant cells. This result suggests that *IRA1* and *IRA2* play partially redundant but distinct roles in regulating cell growth of *sch9Δ/sch9Δ* mutant cells. It has been reported previously that *IRA1* and *IRA2* have similar but not the same functions (Tanaka *et al.* 1990b). Our results resemble those of *ira1* and *ira2* mutations in suppressing the slow growth phenotype of *reg1* mutant cells (Barrett *et al.* 2012). *fst1* and *fst2* are two of the complementation groups of mutants that suppress the *reg1* mutation. *fst1* does not complement *ira1Δ*, and *fst2* does not complement *ira2Δ* for reduced glycogen accumulation and increased agar adhesion. However, *fst1* complements *fst2* in the said phenotypes. The authors concluded that *fst1* is *IRA1* and *fst2* is *IRA2*.

We also analyzed the expression of the *HAP4-lacZ* reporter gene in *ira1Δ*, *ira2Δ*, *sch9Δ ira1Δ*, and *sch9Δ ira2Δ* mutant cells grown in dextrose medium (Figure 5E). We found that *HAP4-lacZ* expression was greatly reduced in these mutants, to the same extent as what was observed in *sns1*, *sns2*, *sch9Δ sns1*, and *sch9Δ sns2* mutant cells. Taken together, our data suggest that *IRA1* and *IRA2* play a largely non-redundant role in inhibiting cell growth in *sch9Δ* mutant cells. To confirm *SNS1* is *IRA2*, we sequenced the *IRA2* gene from a *sns1* mutant and found a frameshift mutation in the codon for serine residue 1870 (Figure 5F). The deletion of the nucleotide C from codon TCT to TT leads to a stop codon almost right after the mutation. Ira2 is a GTPase-activating protein for Ras1 and Ras2, with its Ras GTPase-activating domain being comprised of amino acid residues 1651–1989. This mutation in *IRA2* truncates this domain and helps to explain that *sns1* acts like a total-loss-of-function allele of *IRA2* (Figures 2, 3, and 5).

Mutations in genes encoding components of the PKA signaling pathway affect the expression of *lacZ* reporter genes under the control of *ADR1*, *CAT8*, and/or *HAP4* promoters

Ira1 and Ira2 are GTPase-activating proteins of Ras1 and Ras2 and function as negative regulators of the Ras/PKA signaling pathway (Tanaka *et al.* 1990a, 1991). Gpb1 and Gpb2 interact with Ira1/2 and indirectly inhibit Ras1/2 by promoting the stability of Ira1/2 (Harashima *et al.* 2006). Our data show a clear correlation between the degree of suppression of *sch9Δ* mutant growth defects and reduced expression of *HAP4-lacZ* reporter genes caused by mutations in *GPB1*, *GPB2*, *IRA1*, *IRA2*, and *MCK1*. Activation of PKA signaling is known to suppress the growth defects of *sch9Δ* mutant cells (Toda *et al.* 1988). These results raise the possibility that PKA may inhibit the expression of *HAP4*, *CAT8*, and *ADR1*. The effect of *sns1* and *sns2* mutations on *ADR1* expression is consistent with the reported finding that the expression of an *ADR1-lacZ* reporter gene in dextrose-grown cells is reduced by 9.9-fold due to *bcy1Δ*, which constitutively activates PKA (Dombek and Young 1997).

We decided to determine the effect of a PKA mutation on the expression of *lacZ* reporter genes under the control of these three gene promoters. PKA has three functionally redundant catalytic subunits, Tpk1, Tpk2, and Tpk3 (Toda *et al.* 1987a). A triple deletion in *TPK1/2/3* is lethal, which can be suppressed by a *yak1Δ* mutation (Garrett and Broach 1989). We generated a *tpk1/2/3Δ yak1Δ* quadruple mutant and conducted a β-galactosidase assay in cells grown in dextrose as well as raffinose medium. A *yak1Δ* mutant strain was included as the control and was found to have little to no effect on the expression of these three *lacZ* reporter genes. In dextrose medium, *tpk1/2/3Δ* had a dramatic effect on the expression of the *CAT8*, *ADR1*, and *HAP4* reporter genes and increased their expression by 54-, 6.5-, and 28-fold, respectively (Figure 6). In raffinose medium, *tpk1/2/3Δ* increased *HAP4-lacZ* expression by 3.6-fold, while it had little effect on the expression of *CAT8-lacZ* and *ADR1-lacZ* reporter genes. In contrast, constitutive activation of PKA activity due to a *bcy1Δ* mutation or a *pde1Δ pde2Δ* double mutation resulted in reduced expression of the *HAP4-lacZ* reporter gene in both dextrose and raffinose-grown cells. *bcy1Δ* and *pde1Δ pde2Δ* mutant cells are known to have growth defects on non-fermentable carbon sources (Nikawa *et al.* 1987; Toda *et al.* 1987b), which may be explained by a stronger reduction in *HAP4* expression, and possibly *CAT8* and *ADR1* well, than what is observed in *ira1* and *ira2* single mutant cells. Together, these data indicate that PKA is a strong negative regulator of the expression of *ADR1*, *CAT8*, and *HAP4* under glucose repression conditions.

Mutations in *YAK1* and *PDE2* partially suppress the growth defects of *sch9Δ* mutant cells

IRA1, *IRA2*, *GPB1*, and *GPB2* are negative regulators of Ras1 and Ras2. Mutations in *RAS2* lead to growth defects on nonfermentable carbon sources (Tatchell *et al.* 1985; Fasano *et al.* 1988). It has been suggested that Ras2 can regulate mitochondrial biogenesis and function via both PKA-dependent and independent mechanisms (Hlavata *et al.* 2003; Hlavata and Nystrom 2003). We sought

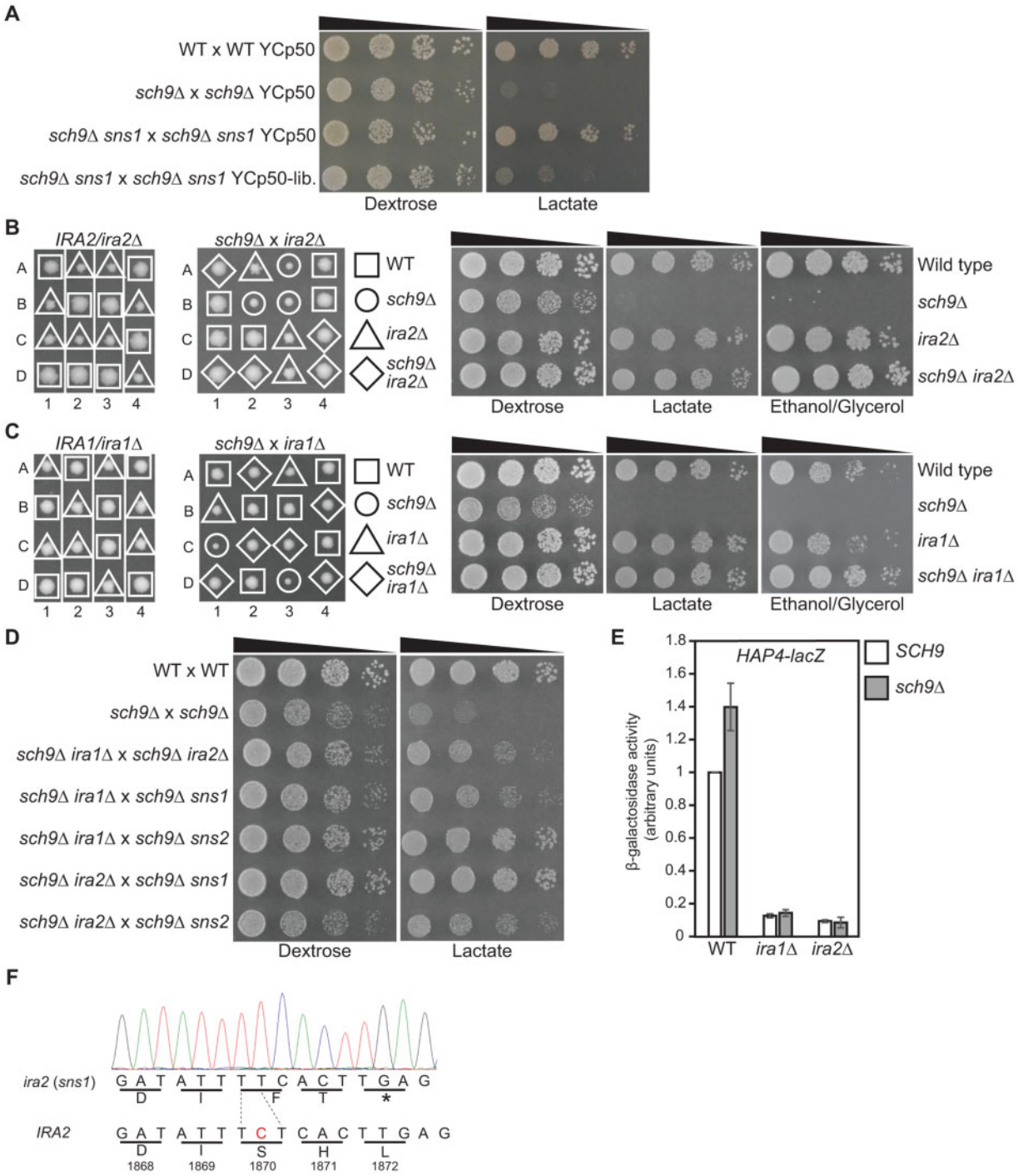

Figure 5 *SNS1* and *SNS2* are *IRA2* and *IRA1*, respectively. (A) A *sns1* mutation is complemented by a genomic DNA library plasmid. Wild type (BY4741 × BY4742), *sch9***Δ** × *sch9***Δ** (PPY745), and *sch9***Δ** *sns1* × *sch9***Δ** *sns1* (PPY741) mutant strains were transformed with control vector YCp50 or the *sns1*-complementing library plasmid, YCp50-lib. (pPP322). Transformants were serially diluted and spotted on YNBcasD (Dextrose) and YNBcasL (Lactate) plates. (B) Tetrad analysis of *IRA2*/*ira2***Δ** (ZLY6578, left panel) and *ira2***Δ** (ZLY6601) × *sch9***Δ** (ZLY6649) (middle panel) on YPD plates. Wild type (BY4741) and isogenic *sch9***Δ** (ZLY6649), *ira2***Δ** (ZLY6609), and *sch9***Δ** *ira2***Δ** (ZLY6661) mutant strains were serially diluted and spotted on YPD, YPL, and YPEG plates (right panel). (C) Tetrad analysis of *IRA1*/*ira1***Δ** (ZLY6656, left panel) and *sch9***Δ** (ZLY6649) × *ira1***Δ** (ZLY6648) (middle panel) on YPD plates. Wild type (BY4741) and isogenic *sch9***Δ** (ZLY6650), *ira1***Δ** (ZLY6648), and *sch9***Δ** *ira1***Δ** (PPY754) mutant strains were serially diluted and spotted on YPD, YPL, and YPEG plates (right panel). (D) Diploid strains obtained from the crossings among *sch9***Δ** *ira1***Δ** (PPY755), *sch9***Δ** *ira2***Δ** (ZLY6661), *sch9***Δ** *sns1* (PPY733, PPY734), and *sch9***Δ** *sns2* (ZLY6619, ZLY6626) mutant strains as indicated were serially diluted and spotted on YPD and YPL plates. BY4741 × BY4742 and *sch9***Δ** × *sch9***Δ** (PPY745) strains were included as controls. (E) β-galactosidase activities of a *HAP4-lacZ* reporter gene in wild type (BY4741), *ira1***Δ** (ZLY6647), and *ira2***Δ** (ZLY6609) mutant strains with or without an *sch9***Δ** deletion mutation grown in YNBcas5D medium. The *HAP4-lacZ* reporter gene activity in the wild type strain is set as 1. (F) *IRA2* from *sns1* mutant cells has a frameshift mutation. The chromatogram shows the sequence of *IRA2* containing the frameshift mutation from a *sns1* mutant. The nucleotide C missing in the *IRA2* gene from the *sns1* mutant was highlighted in red in the wild type *IRA2* sequence.

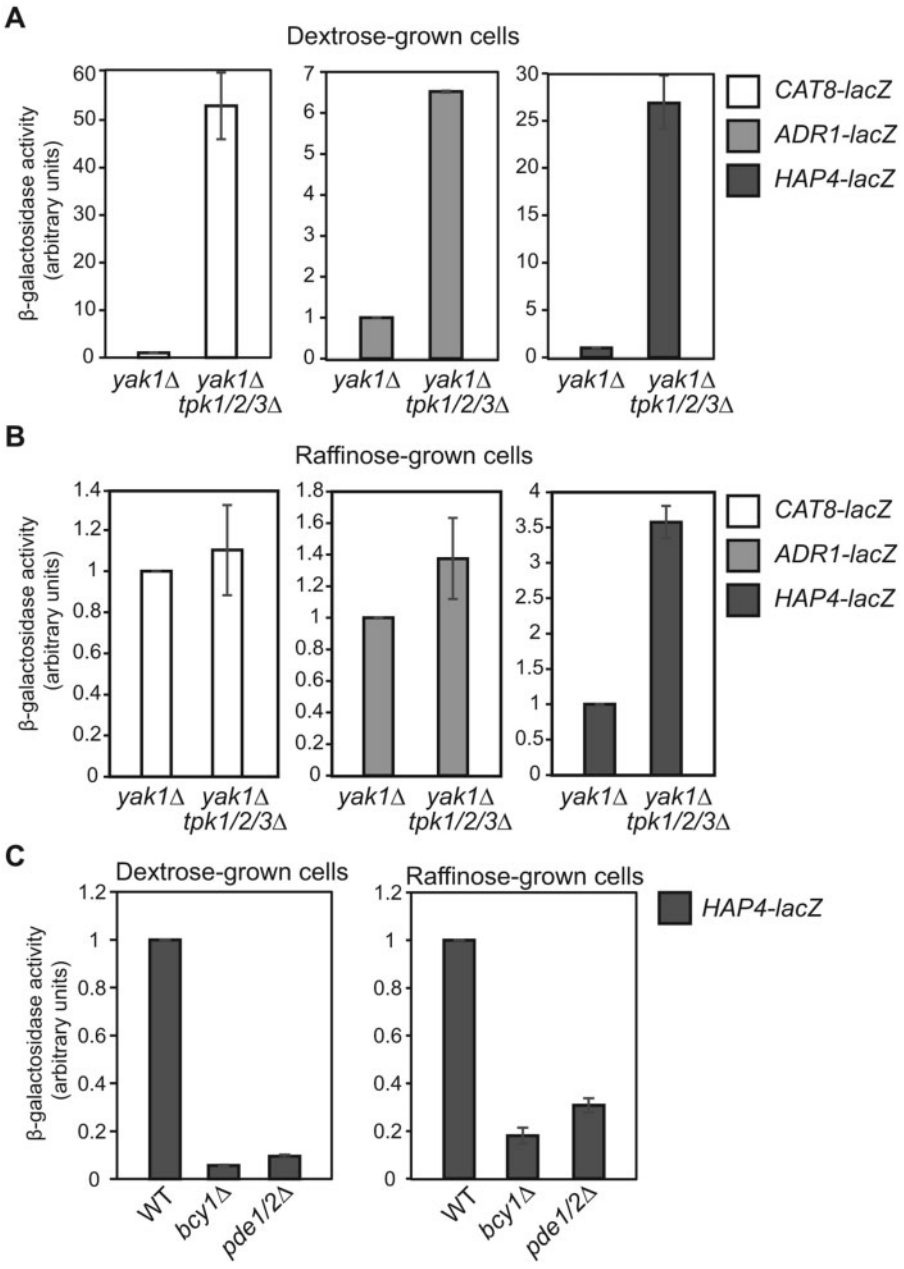

Figure 6 Mutations in genes encoding components of the PKA signaling pathway affect the expression of *lacZ* reporter genes under the control of *ADR1*, *CAT8*, and/or *HAP4* promoters. (A-B) β-galactosidase activities of *CAT8-lacZ*, *ADR1-lacZ*, and *HAP4-lacZ* reporter genes in *yak1*Δ (ZLY4313) and *yak1*Δ *tpk1/2/3*Δ (ZLY5023) mutant strains grown in YNBcas5D (A) and YNBcasR (B) medium. β-galactosidase activity from each of the three reporter genes in the *yak1*Δ strain was set as 1, respectively. (C) β-galactosidase activities of a *HAP4-lacZ* reporter gene in wild type (BY4741), *bcy1*Δ (ZLY6715), and *pde1*Δ *pde2*Δ (PPY776) mutant cells grown in dextrose and raffinose medium. The activity of *HAP4-lacZ* in wild type cells was set as 1.

to determine whether the suppression of an *sch9*Δ mutant's growth defects on non-fermentable carbon source is mediated through PKA-dependent or independent Ras2 functions. To that end, we analyzed the effect of mutations in genes functioning in the PKA pathway downstream of Ras1 and Ras2. Since *bcy1*Δ and *pde1*Δ *pde2*Δ lead to growth defects on non-fermentable carbon sources and may complicate the analysis of *sch9*Δ suppression, we determined the effect of single gene mutations of *YAK1*, *PDE1*, and *PDE2* on *sch9*Δ suppression by generating double mutant strains via tetrad analysis. We found that *yak1*Δ and *pde2*Δ, but not *pde1*Δ, partially suppressed the growth defect of *sch9*Δ mutant cells on dextrose dissection plate. A cell growth assay via serial dilution confirmed that *yak1*Δ and *pde2*Δ single mutations partially suppressed the growth defects of *sch9*Δ mutant cells on both dextrose and lactate medium (Figure 7, A and B). Our results suggest that the suppression of growth defects of *sch9*Δ mutant cells on dextrose medium and non-fermentable carbon sources is mediated at least through the activation of the PKA pathway. We cannot exclude the possibility that activation of PKA-independent Ras2 function(s) may also contribute to *sch9*Δ suppression in some of the suppressor mutants.

Chronological lifespan extension due to *sch9*Δ is reversed by an *ira2* mutation

*sch9*Δ mutant cells have been previously shown to extend chronological lifespan (Fabrizio *et al.* 2001; Longo 2003; Wei *et al.* 2008).

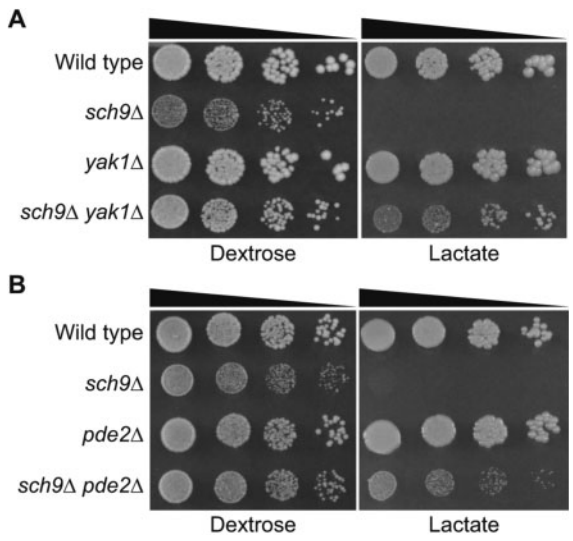

Figure 7 Mutations in *YAK1* and *PDE2* partially suppress the growth defects of *sch9Δ* mutant cells. (A) *sch9Δ* suppression by *yak1Δ*. Wild type (BY4741) and isogenic *sch9Δ* (ZLY6650), *yak1Δ* (ZLY4313), and *sch9Δ yak1Δ* (ZLY6707) mutant strains were serially diluted and spotted on dextrose (YPD) and lactate (YPL) medium. (B) *sch9Δ* suppression by *pde2Δ*. Wild type (BY4741) and isogenic *sch9Δ* (ZLY6650), *pde2Δ* (ZLY4368), and *sch9Δ pde2Δ* (PPY758) mutant cells were serially diluted and spotted on YPD and YPL plates.

Mutations in *IRA2* reverse the growth defects of *sch9Δ* mutant cells. We wanted to determine the effect of an *ira2* mutation on chronological lifespan in *sch9Δ* mutant cells. To that end, we generated a survival curve of wild type, *sch9Δ*, *ira2*, and *sch9Δ ira2* diploid strains grown in raffinose media (Figure 8). Cell growth in raffinose medium mimics glucose limitation conditions, which accounts for the relatively long chronological life span in wild type cells. As expected, *sch9Δ* mutant cells had better survival than wild type. Both *ira2* and *sch9Δ ira2* mutant strains showed a significant decrease in cell survival. Mutations in genes in the PKA signaling pathway that inhibit or activate PKA lead to a longer or shorter chronological lifespan, respectively (Fabrizio *et al.* 2001, 2003; Longo 2003). Reductions in Sch9 activity and PKA pathway signaling have been reported to extend life span in an additive manner (Wei *et al.* 2008). *ira2* mutants are known to have increased Ras/PKA pathway activity (Tanaka *et al.* 1990b). Together, these data suggest that activation of PKA signaling due to an *ira2* mutation antagonizes lifespan extension in *sch9Δ* mutant cells.

Discussion

Deletion of *SCH9* has been previously reported to cause a slow growth phenotype on dextrose medium, but the growth phenotypes demonstrated on non-fermentable carbon sources are inconsistent. In this report, we propose that the rapid accumulation of suppressor mutations in *sch9Δ* mutant cells could account for the discrepancies in the published results. All 18 of the isolated spontaneously arising, recessive mutations that suppressed the growth defects of *sch9Δ* mutant cells were proposed to be in either *IRA1* or *IRA2*. Using genetic techniques, we also found that mutations in *GPB1*, *GPB2*, and *MCK1* suppress the growth defects of *sch9Δ* mutant cells in both dextrose medium and non-fermentable carbon sources. Many studies on the cellular functions of Sch9 employed strains of the W303 and S288c backgrounds, which we also used in this report. The discrepancies in the published literature regarding changes in the expression of *HAP4*, genes encoding mitochondrial proteins, stress-responsive genes, and oxygen consumption due to *sch9* mutations may be attributed to the presence or absence of *sch9* suppressor mutations (Crauwels *et al.* 1997; Fabrizio *et al.* 2003; Pedruzzi *et al.* 2003; Jorgensen *et al.* 2004; Roosen *et al.* 2005; Lavoie and Whiteway 2008; Smets *et al.* 2008; Pan and Shadel 2009; Pan *et al.* 2011; Teixeira *et al.* 2014). It is also possible that the use of other strain backgrounds, growth conditions, and growth phase could account for the discrepancies. By removing the complication of *sch9Δ* suppressor mutations, future studies will help reconcile the reported conflicting functions of Sch9 and may uncover novel functions for Sch9.

Fast accumulation of suppressor mutations in *sch9Δ* mutant cells was so prevalent that it was difficult for us to maintain *sch9Δ* mutant strains. It is not clear why there are frequent spontaneous mutations in *IRA1* and *IRA2* loci, which were calculated to arise at a frequency of 1.1×10^{-3} (Halme *et al.* 2004). Halme et al. further showed that missense mutations and single base-pair deletions or insertions are behind the high-frequency genetic events in *IRA1* and *IRA2* genes. During the review of this manuscript, we were brought to the attention of a report by van Leeuwen et al., showing that *IRA2* is a candidate suppressor gene in a spontaneous *sch9Δ* suppressor mutant (2016). *sch9Δ* cells are slow-growing on dextrose media, and the suppressor mutants grow considerably faster and quickly take over the population. We found it was necessary to purify *sch9Δ* strains right before they were used in each experiment. When purified *sch9Δ* mutant strains are grown in liquid cultures, it is also important to save small aliquots of cultured cells and examine their growth on dextrose plate medium to determine the extent of "contamination" by spontaneous suppressor mutants. Since most suppressor mutations we isolated were recessive, we propose that *sch9Δ* homozygous diploid mutant strains should be used for studies on the cellular functions of Sch9. The other alternative is to use analog-sensitive *sch9* alleles, but the accumulation of suppressor mutations is still expected to take place. Given that all 18 recessive suppressor mutations we isolated were in either *IRA1* or *IRA2*, another option is to use *sch9Δ* haploid mutant strains carrying an extra copy of *IRA1* and *IRA2*. However, extra copies of *IRA1* and *IRA2* may reduce the activity of the Ras/PKA signaling pathway, which could skew conclusions on the cellular functions for Sch9.

Suppression of the growth defects of *sch9Δ* mutants by *IRA1*, *IRA2*, *GPB1*, and *GPB2* is consistent with the notion that PKA and Sch9 play overlapping roles in regulating cell growth in response to nutrient conditions. It has been reported that activation of PKA can suppress the mutant phenotype of *sch9Δ* and vice versa. *IRA1* and *IRA2* are GTPase-activating proteins of Ras1/2 and function as negative regulators of the Ras/PKA signaling pathway. Gpb1/2 are negative regulators of PKA signaling by inhibiting Ras, directly regulating PKA, and/or by other means (reviewed in Broach 2012). Therefore, the suppression of growth defects of *sch9Δ* mutant cells due to mutations in *IRA1/2* and *GPB1/2* can be explained by increased activity of Ras/PKA signaling. The mechanism behind *mck1Δ* suppression of *sch9Δ* is less clear. Mck1 was originally characterized for its role in meiosis and chromosome segregation (Neigeborn and Mitchell 1991; Shero and Hieter 1991). It has also been shown that Mck1 may be required for the activity of Msn2/4 (Hirata *et al.* 2003; Sadeh *et al.* 2011; Gutin *et al.* 2015, 2019). Mutations in *IRA2*, *MCK1*, *MSN2/4*, *YAK1*, and *RIM15* lead to a similar transcriptional response of a *HSP12* reporter, while *sch9Δ* has an opposite effect (Gutin *et al.* 2015, 2019). Mutations in *YAK1*, *RIM15*, and *MSN2/4* have also been reported to suppress cell

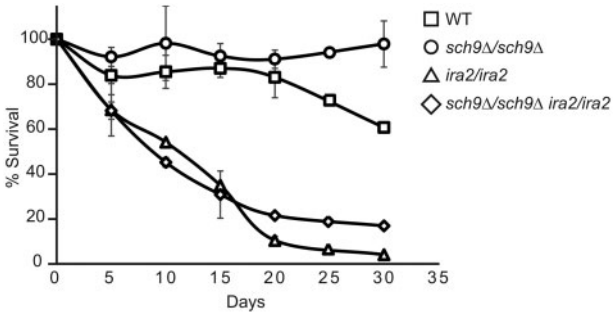

Figure 8 Chronological lifespan extension due to an *sch9*Δ mutation is reversed by an *ira2* mutation. Wild type (BY4741 × BY4742) and isogenic *sch9*Δ × *sch9*Δ (PPY745), *ira2* × *ira2* (PPY737), and *sch9*Δ *ira2* × *sch9*Δ *ira2* (PPY741) mutant strains were grown in YPR media for 30 days after cultures reached saturation. Percent survival was calculated using colony forming assay at the indicated time points. Errors bars represent the standard deviation of the results from two independent experiments.

lethality associated with a *tpk1/2/3* triple mutation (reviewed in Broach 2012). It is conceivable that *mck1*Δ may suppress the growth defects of *sch9*Δ through the Ras/PKA pathway. A potential role of Mck1 in PKA signaling or in another pathway will be examined in future studies.

The effect of *sch9*Δ, *ira1*Δ, *ira2*Δ, *gpb1/2*Δ, and *mck1*Δ on the expression of *HAP4*, *ADR1*, and *CAT8* presents an interesting paradox between cell growth and gene expression. Hap4, Adr1, and Cat8 are global transcriptional activators that are important for the expression of genes involved in gluconeogenesis, the glyoxylate cycle, mitochondrial biogenesis, and/or oxidative metabolism. *sch9*Δ mutants are unable to utilize non-fermentable carbon sources for growth, which suggests a decrease in the expression of genes involved in respiratory metabolism and gluconeogenesis. Instead, however, *sch9*Δ increases the expression of genes encoding key transcriptional activators that are required for the utilization of non-fermentable carbon sources. On the other hand, *sch9*Δ *ira1* and *sch9*Δ *ira2* mutant strains can grow robustly on non-fermentable carbon sources, but they exhibit reduced promoter activity of these three transcriptional activators. One possibility may have to do with greatly increased expression of *HAP4*, *CAT8*, and *ADR1* genes under glucose limitation conditions (Figure 3A). Due to high levels of transcripts, a large reduction in the promoter activity in *sch9*Δ *ira1* and *sch9*Δ *ira2* mutant cells may not translate into reduced protein levels to the same degree. Functional redundancy may also help explain the lack of growth defects in *sch9*Δ *ira1* and *sch9*Δ *ira2* strains on non-fermentable carbon sources. For example, in raffinose-grown cells, *CAT8* expression is reduced in these two mutant cells compared with wild type. However, the function of Cat8 is redundant with other transcriptional activators and its downregulation in these mutants may not prevent cells from utilizing non-fermentable carbon sources (reviewed in Schuller 2003; Turcotte *et al.* 2010). It is also possible that increased expression of *HAP4*, *CAT8*, and *ADR1* due to *sch9*Δ may be an adaptative response to cell growth defects. It is important to note that a large difference in transcriptional response determined by the *lacZ* reporter genes is not translated to the same degree of change in HA-tagged Cat8 or Hap4 determined by Western blotting (Figure 3). This may suggest that translation of *CAT8* and *HAP4* transcripts may be different from that of *lacZ*. It is also possible that Cat8 and Hap4 may be subjected to post-translational controls that are not available to the *lacZ* protein.

The transcriptional response mediated by PKA has been proposed to be conducted mainly through Msn2/4, Gis1, and Rim15 (Roosen *et al.* 2005; Broach 2012; Pfanzagl *et al.* 2018). Our data show that PKA is a negative regulator of *HAP4*, *CAT8*, and *ADR1* (Figure 6). The expression of *ADR1* is under negative control by PKA signaling (Dombek and Young 1997). Downregulation of the expression of these three genes in *ira1*, *ira2*, and *gpb1/2* mutants is likely to be caused by the activation of PKA signaling (Figures 3–5). How does PKA regulate the expression of *HAP4*, *ADR1*, and *CAT8*? Both *HAP4* and *CAT8* are subject to Mig1-dependent downregulation under glucose repression conditions (reviewed in Schuller 2003; Turcotte *et al.* 2010; Broach 2012). However, it is unknown whether the effect is direct or indirect. Expression of *HAP4* is dependent on Hap1 and is subject to auto-regulatory control (Zhang *et al.* 2017). Increased expression of *CAT8* is dependent on Hap2/3/4/5 under glucose limitation conditions (Rahner *et al.* 1996). Apart from the findings from this study and others that PKA negatively regulates *ADR1* expression, transcriptional regulation of *ADR1* is largely unknown. Future studies will be needed to understand the molecular mechanisms underlying the regulation of *HAP4*, *ADR1*, and *CAT8* by PKA.

Acknowledgments

The authors thank Manika Bhondeley and Savannah Rappold for technical support and Tammy Pracheil Bavaret for editing this manuscript.

Funding

This study was supported by a grant from the U.S. National Institutes of Health (1R15GM121998-01).

Conflicts of interest

Authors have no conflict of interest to declare.

Literature cited

Amberg DC, Burke DJ, Strathern JN. 2005. Methods in Yeast Genetics: A Cold Spring Harbor Laboratory Course Manual. New York, NY: Cold Spring Harbor Laboratory, Cold Spring Harbor.

Barrett L, Orlova M, Maziarz M, Kuchin S. 2012. Protein kinase A contributes to the negative control of Snf1 protein kinase in *Saccharomyces cerevisiae*. Eukaryot Cell. 11:119–128.

Bianchi MW, Plyte SE, Kreis M, Woodgett JR. 1993. A *Saccharomyces cerevisiae* protein-serine kinase related to mammalian glycogen synthase kinase-3 and the *Drosophila melanogaster* gene *shaggy* product. Gene. 134:51–56.

Broach JR. 2012. Nutritional control of growth and development in yeast. Genetics. 192:73–105.

Budhwar R, Fang G, Hirsch JP. 2011. Kelch repeat proteins control yeast PKA activity in response to nutrient availability. Cell Cycle. 10:767–770.

Burnett PE, Barrow RK, Cohen NA, Snyder SH, Sabatini DM. 1998. RAFT1 phosphorylation of the translational regulators p70 S6 kinase and 4E-BP1. Proc Natl Acad Sci U S A. 95:1432–1437.

Burtner CR, Murakami CJ, Kennedy BK, Kaeberlein M. 2009. A molecular mechanism of chronological aging in yeast. Cell Cycle. 8: 1256–1270.

Cooper TG. 2002. Transmitting the signal of excess nitrogen in *Saccharomyces cerevisiae* from the Tor proteins to the GATA factors: connecting the dots. FEMS Microbiol Rev. 26:223–238.

Crauwels M, Donaton MC, Pernambuco MB, Winderickx J, de Winde JH, *et al.* 1997. The Sch9 protein kinase in the yeast *Saccharomyces cerevisiae* controls cAPK activity and is required for nitrogen

activation of the fermentable-growth-medium-induced (FGM) pathway. Microbiology. 143:2627–2637.

Denis CL, Audino DC. 1991. The CCR1 (SNF1) and SCH9 protein kinases act independently of cAMP-dependent protein kinase and the transcriptional activator ADR1 in controlling yeast *ADH2* expression. Mol Gen Genet. 229:395–399.

Deutschbauer AM, Williams RM, Chu AM, Davis RW. 2002. Parallel phenotypic analysis of sporulation and postgermination growth in *Saccharomyces cerevisiae*. Proc Natl Acad Sci U S A. 99: 15530–15535.

Dombek KM, Young ET. 1997. Cyclic AMP-dependent protein kinase inhibits *ADH2* expression in part by decreasing expression of the transcription factor gene *ADR1*. Mol Cell Biol. 17:1450–1458.

Enyenihi AH, Saunders WS. 2003. Large-scale functional genomic analysis of sporulation and meiosis in *Saccharomyces cerevisiae*. Genetics. 163:47–54.

Fabrizio P, Liou LL, Moy VN, Diaspro A, Valentine JS, *et al.* 2003. *SOD2* functions downstream of Sch9 to extend longevity in yeast. Genetics. 163:35–46.

Fabrizio P, Pozza F, Pletcher SD, Gendron CM, Longo VD. 2001. Regulation of longevity and stress resistance by Sch9 in yeast. Science. 292:288–290.

Fasano O, Crechet JB, De Vendittis E, Zahn R, Feger G, *et al.* 1988. Yeast mutants temperature-sensitive for growth after random mutagenesis of the chromosomal *RAS2* gene and deletion of the *RAS1* gene. Embo J. 7:3375–3383.

Forsburg SL, Guarente L. 1989. Identification and characterization of HAP4: a third component of the CCAAT-bound HAP2/HAP3 heteromer. Genes Dev. 3:1166–1178.

Garrett S, Broach J. 1989. Loss of Ras activity in *Saccharomyces cerevisiae* is suppressed by disruptions of a new kinase gene, *YAK1*, whose product may act downstream of the cAMP-dependent protein kinase. Genes Dev. 3:1336–1348.

Geyskens I, Kumara S, Donaton M, Bergsma J, Thevelein J, *et al.* 2001. Expression of mammalian PKB partially complements deletion of the yeast protein kinase Sch9. In: Proceedings of NATO Conference. Amsterdam, Netherlands: IOS Press. p. 117–126.

Gietz D, St Jean A, Woods RA, Schiestl RH. 1992. Improved method for high efficiency transformation of intact yeast cells. Nucleic Acids Res. 20:1425.

Gutin J, Joseph-Strauss D, Sadeh A, Shalom E, Friedman N. 2019. Genetic screen of the yeast environmental stress response dynamics uncovers distinct regulatory phases. Mol Syst Biol. 15: e8939.

Gutin J, Sadeh A, Rahat A, Aharoni A, Friedman N. 2015. Condition-specific genetic interaction maps reveal crosstalk between the cAMP/PKA and the HOG MAPK pathways in the activation of the general stress response. Mol Syst Biol. 11:829.

Halme A, Bumgarner S, Styles C, Fink GR. 2004. Genetic and epigenetic regulation of the *FLO* gene family generates cell-surface variation in yeast. Cell. 116:405–415.

Harashima T, Anderson S, Yates JR, 3rd, Heitman J. 2006. The kelch proteins Gpb1 and Gpb2 inhibit Ras activity via association with the yeast RasGAP neurofibromin homologs Ira1 and Ira2. Mol Cell. 22:819–830.

Harashima T, Heitman J. 2002. The Galpha protein Gpa2 controls yeast differentiation by interacting with kelch repeat proteins that mimic Gbeta subunits. Mol Cell. 10:163–173.

Hardy TA, Wu D, Roach PJ. 1995. Novel *Saccharomyces cerevisiae* gene, *MRK1*, encoding a putative protein kinase with similarity to mammalian glycogen synthase kinase-3 and *Drosophila* Zeste-White3/Shaggy. Biochem Biophys Res Commun. 208:728–734.

Hedges D, Proft M, Entian KD. 1995. *CAT8*, a new zinc cluster-encoding gene necessary for derepression of gluconeogenic enzymes in the yeast *Saccharomyces cerevisiae*. Mol Cell Biol. 15:1915–1922.

Hlavata L, Aguilaniu H, Pichova A, Nystrom T. 2003. The oncogenic *RAS2*(val19) mutation locks respiration, independently of PKA, in a mode prone to generate ROS. Embo J. 22: 3337–3345.

Hlavata L, Nystrom T. 2003. Ras proteins control mitochondrial biogenesis and function in *Saccharomyces cerevisiae*. Folia Microbiol (Praha). 48:725–730.

Hirata Y, Andoh T, Asahara T, Kikuchi A. 2003. Yeast glycogen synthase kinase-3 activates Msn2p-dependent transcription of stress responsive genes. Mol Biol Cell. 14:302–312.

Huber A, Bodenmiller B, Uotila A, Stahl M, Wanka S, *et al.* 2009. Characterization of the rapamycin-sensitive phosphoproteome reveals that Sch9 is a central coordinator of protein synthesis. Genes Dev. 23:1929–1943.

Huber A, French SL, Tekotte H, Yerlikaya S, Stahl M, *et al.* 2011. Sch9 regulates ribosome biogenesis via Stb3, Dot6 and Tod6 and the histone deacetylase complex RPD3L. EMBO J. 30:3052–3064.

Jorgensen P, Nishikawa JL, Breitkreutz BJ, Tyers M. 2002. Systematic identification of pathways that couple cell growth and division in yeast. Science. 297:395–400.

Jorgensen P, Rupes I, Sharom JR, Schneper L, Broach JR, *et al.* 2004. A dynamic transcriptional network communicates growth potential to ribosome synthesis and critical cell size. Genes Dev. 18: 2491–2505.

Kaeberlein M, Powers RW, Steffen KK, Westman EA, Hu D, *et al.* 2005. Regulation of yeast replicative life span by TOR and Sch9 in response to nutrients. Science. 310:1193–1196.

Kraakman L, Lemaire K, Ma P, Teunissen AW, Donaton MC, *et al.* 1999. A *Saccharomyces cerevisiae* G-protein coupled receptor, Gpr1, is specifically required for glucose activation of the cAMP pathway during the transition to growth on glucose. Mol Microbiol. 32:1002–1012.

Lavoie H, Whiteway M. 2008. Increased respiration in the sch9Delta mutant is required for increasing chronological life span but not replicative life span. Eukaryot Cell. 7:1127–1135.

Lee J, Moir RD, Willis IM. 2009. Regulation of RNA polymerase III transcription involves *SCH9*-dependent and *SCH9*-independent branches of the target of rapamycin (TOR) pathway. J Biol Chem. 284:12604–12608.

Lippman SI, Broach JR. 2009. Protein kinase A and TORC1 activate genes for ribosomal biogenesis by inactivating repressors encoded by *Dot6* and its homolog *Tod6*. Proc Natl Acad Sci U S A. 106:19928–19933.

Liu Z, Butow RA. 1999. A transcriptional switch in the expression of yeast tricarboxylic acid cycle genes in response to a reduction or loss of respiratory function. Mol Cell Biol. 19:6720–6728.

Loewith R, Hall MN. 2011. Target of rapamycin (TOR) in nutrient signaling and growth control. Genetics. 189:1177–1201.

Longo VD. 2003. The Ras and Sch9 pathways regulate stress resistance and longevity. Exp Gerontol. 38:807–811.

Lorenz MC, Pan X, Harashima T, Cardenas ME, Xue Y, *et al.* 2000. The G protein-coupled receptor Gpr1 is a nutrient sensor that regulates pseudohyphal differentiation in *Saccharomyces cerevisiae*. Genetics. 154:609–622.

Morano KA, Thiele DJ. 1999. The Sch9 protein kinase regulates Hsp90 chaperone complex signal transduction activity in vivo. Embo J. 18:5953–5962.

Neigeborn L, Mitchell AP. 1991. The yeast *MCK1* gene encodes a protein kinase homolog that activates early meiotic gene expression. Genes Dev. 5:533–548.

Nikawa J, Sass P, Wigler M. 1987. Cloning and characterization of the low-affinity cyclic AMP phosphodiesterase gene of *Saccharomyces cerevisiae*. Mol Cell Biol. 7:3629–3636.

Pan Y, Schroeder EA, Ocampo A, Barrientos A, Shadel GS. 2011. Regulation of yeast chronological life span by TORC1 via adaptive mitochondrial ROS signaling. Cell Metab. 13:668–678.

Pan Y, Shadel GS. 2009. Extension of chronological life span by reduced TOR signaling requires down-regulation of Sch9p and involves increased mitochondrial OXPHOS complex density. Aging (Albany NY). 1:131–145.

Pascual-Ahuir A, Proft M. 2007. The Sch9 kinase is a chromatin-associated transcriptional activator of osmostress-responsive genes. Embo J. 26:3098–3108.

Pedruzzi I, Dubouloz F, Cameroni E, Wanke V, Roosen J, *et al.* 2003. TOR and PKA signaling pathways converge on the protein kinase Rim15 to control entry into G0. Mol Cell. 12:1607–1613.

Pfanzagl V, Gorner W, Radolf M, Parich A, Schuhmacher R, *et al.* 2018. A constitutive active allele of the transcription factor Msn2 mimicking low PKA activity dictates metabolic remodeling in yeast. Mol Biol Cell. 29:2848–2862.

Phan VT, Ding VW, Li F, Chalkley RJ, Burlingame A, *et al.* 2010. The RasGAP proteins Ira2 and neurofibromin are negatively regulated by Gpb1 in yeast and ETEA in humans. Mol Cell Biol. 30: 2264–2279.

Plank M, Perepelkina M, Muller M, Vaga S, Zou X, *et al.* 2020. Chemical genetics of AGC-kinases reveals shared targets of Ypk1, Protein Kinase A and Sch9. Mol Cell Proteomics.

Prusty R, Keil RL. 2004. *SCH9*, a putative protein kinase from *Saccharomyces cerevisiae*, affects *HOT1*-stimulated recombination. Mol Genet Genomics. 272:264–274.

Puziss JW, Hardy TA, Johnson RB, Roach PJ, Hieter P. 1994. *MDS1*, a dosage suppressor of an *mck1* mutant, encodes a putative yeast homolog of glycogen synthase kinase 3. Mol Cell Biol. 14:831–839.

Rahner A, Scholer A, Martens E, Gollwitzer B, Schuller HJ. 1996. Dual influence of the yeast Cat1p (Snf1p) protein kinase on carbon source-dependent transcriptional activation of gluconeogenic genes by the regulatory gene *CAT8*. Nucleic Acids Res. 24: 2331–2337.

Randez-Gil F, Bojunga N, Proft M, Entian KD. 1997. Glucose derepression of gluconeogenic enzymes in *Saccharomyces cerevisiae* correlates with phosphorylation of the gene activator Cat8p. Mol Cell Biol. 17:2502–2510.

Roosen J, Engelen K, Marchal K, Mathys J, Griffioen G, *et al.* 2005. PKA and Sch9 control a molecular switch important for the proper adaptation to nutrient availability. Mol Microbiol. 55:862–880.

Sadeh A, Movshovich N, Volokh M, Gheber L, Aharoni A. 2011. Fine-tuning of the Msn2/4-mediated yeast stress responses as revealed by systematic deletion of Msn2/4 partners. Mol Biol Cell. 22:3127–3138.

Schmelzle T, Beck T, Martin DE, Hall MN. 2004. Activation of the RAS/cyclic AMP pathway suppresses a TOR deficiency in yeast. Mol Cell Biol. 24:338–351.

Schuller HJ. 2003. Transcriptional control of nonfermentative metabolism in the yeast *Saccharomyces cerevisiae*. Curr Genet. 43: 139–160.

Shero JH, Hieter P. 1991. A suppressor of a centromere DNA mutation encodes a putative protein kinase (*MCK1*). Genes Dev. 5:549–560.

Smets B, De Snijder P, Engelen K, Joossens E, Ghillebert R, *et al.* 2008. Genome-wide expression analysis reveals TORC1-dependent and -independent functions of Sch9. FEMS Yeast Res. 8:1276–1288.

Sobko A. 2006. Systems biology of AGC kinases in fungi. Sci Stke. 2006:re9.

Soulard A, Cremonesi A, Moes S, Schutz F, Jeno P, *et al.* 2010. The rapamycin-sensitive phosphoproteome reveals that TOR controls protein kinase A toward some but not all substrates. Mol Biol Cell. 21:3475–3486.

Swinnen E, Wilms T, Idkowiak-Baldys J, Smets B, Snijder PD, *et al.* 2014. The protein kinase Sch9 is a key regulator of sphingolipid metabolism in *Saccharomyces cerevisiae*. Mol Biol Cell. 25: 196–211.

Tanaka K, Lin BK, Wood DR, Tamanoi F. 1991. IRA2, an upstream negative regulator of RAS in yeast, is a RAS GTPase-activating protein. Proc Natl Acad Sci U S A. 88:468–472.

Tanaka K, Nakafuku M, Satoh T, Marshall MS, Gibbs JB, *et al.* 1990a. S. cerevisiae genes *IRA1* and *IRA2* encode proteins that may be functionally equivalent to mammalian *ras* GTPase activating protein. Cell. 60:803–807.

Tanaka K, Nakafuku M, Tamanoi F, Kaziro Y, Matsumoto K, *et al.* 1990b. *IRA2*, a second gene of *Saccharomyces cerevisiae* that encodes a protein with a domain homologous to mammalian *ras* GTPase-activating protein. Mol Cell Biol. 10: 4303–4313.

Tatchell K, Robinson LC, Breitenbach M. 1985. *RAS2* of *Saccharomyces cerevisiae* is required for gluconeogenic growth and proper response to nutrient limitation. Proc Natl Acad Sci U S A. 82: 3785–3789.

Teixeira V, Medeiros TC, Vilaca R, Moradas-Ferreira P, Costa V. 2014. Reduced TORC1 signaling abolishes mitochondrial dysfunctions and shortened chronological lifespan of Isc1p-deficient cells. Microb Cell. 1:21–36.

Thevelein JM, de Winde JH. 1999. Novel sensing mechanisms and targets for the cAMP-protein kinase A pathway in the yeast *Saccharomyces cerevisiae*. Mol Microbiol. 33:904–918.

Toda T, Cameron S, Sass P, Wigler M. 1988. *SCH9*, a gene of *Saccharomyces cerevisiae* that encodes a protein distinct from, but functionally and structurally related to, cAMP-dependent protein kinase catalytic subunits. Genes Dev. 2:517–527.

Toda T, Cameron S, Sass P, Zoller M, Wigler M. 1987a. Three different genes in S. cerevisiae encode the catalytic subunits of the cAMP-dependent protein kinase. Cell. 50:277–287.

Toda T, Cameron S, Sass P, Zoller M, Scott JD, *et al.* 1987b. Cloning and characterization of *BCY1*, a locus encoding a regulatory subunit of the cyclic AMP-dependent protein kinase in *Saccharomyces cerevisiae*. Mol Cell Biol. 7:1371–1377.

Turcotte B, Liang XB, Robert F, Soontorngun N. 2010. Transcriptional regulation of nonfermentable carbon utilization in budding yeast. FEMS Yeast Res. 10:2–13.

Urban J, Soulard A, Huber A, Lippman S, Mukhopadhyay D, *et al.* 2007. Sch9 is a major target of TORC1 in *Saccharomyces cerevisiae*. Mol Cell. 26:663–674.

van Leeuwen J, Pons C, Mellor JC, Yamaguchi TN, Friesen H, *et al.* 2016. Exploring genetic suppression interactions on a global scale. Science. 354:aag0839.

Wei M, Fabrizio P, Hu J, Ge H, Cheng C, *et al.* 2008. Life span extension by calorie restriction depends on Rim15 and transcription factors downstream of Ras/PKA, Tor, and Sch9. PLoS Genet. 4:e13.

Wei Y, Zheng XF. 2009. Sch9 partially mediates TORC1 signaling to control ribosomal RNA synthesis. Cell Cycle. 8:4085–4090.

Wilms T, Swinnen E, Eskes E, Dolz-Edo L, Uwineza A, *et al.* 2017. The yeast protein kinase Sch9 adjusts V-ATPase assembly/disassembly to control pH homeostasis and longevity in response to glucose availability. PLoS Genet. 13:e1006835.

Wullschleger S, Loewith R, Hall MN. 2006. TOR signaling in growth and metabolism. Cell. 124:471–484.

Yaffe MP, Schatz G. 1984. Two nuclear mutations that block mitochondrial protein import in yeast. Proc Natl Acad Sci U S A. 81: 4819–4823.

Yorimitsu T, Zaman S, Broach JR, Klionsky DJ. 2007. Protein kinase A and Sch9 cooperatively regulate induction of autophagy in *Saccharomyces cerevisiae*. Mol Biol Cell. 18:4180–4189.

Zaman S, Lippman SI, Schneper L, Slonim N, Broach JR. 2009. Glucose regulates transcription in yeast through a network of signaling pathways. Mol Syst Biol. 5:245.

Zaman S, Lippman SI, Zhao X, Broach JR. 2008. How Saccharomyces responds to nutrients. Annu Rev Genet. 42:27–81.

Zhang A, Shen Y, Gao W, Dong J. 2011. Role of Sch9 in regulating Ras-cAMP signal pathway in *Saccharomyces cerevisiae*. FEBS Lett. 585:3026–3032.

Zhang T, Bu P, Zeng J, Vancura A. 2017. Increased heme synthesis in yeast induces a metabolic switch from fermentation to respiration even under conditions of glucose repression. J Biol Chem. 292:16942–16954.

Communicating editor: G. Brown